Trinity College Dublin
Coláiste na Tríonóide, Baile Átha Cliath
The University of Dublin

Collagen deposition, cellular and molecular characterisation of self-assembled tendon constructs grown *in-vitro* from embryonic chick tenocyte cells.

By

Grace Morris

Research Masters in Zoology, January 2025

School of Natural Sciences, Trinity College Dublin

Supervisor: Prof Paula Murphy, Co-Supervisor: Dr Rebecca Rolfe

Declaration:

I declare that this thesis has not been submitted as an exercise for a degree at this or any other university and it is entirely my own work. I agree to deposit this thesis in the University's open access institutional repository or allow the library to do so on my behalf, subject to Irish Copyright Legislation and Trinity College Library conditions of use and acknowledgement. I consent to the examiner retaining a copy of the thesis beyond the examining period, should they so wish (EU GDPR May 2018).

Grace Morris

June, 2024

Abstract

Tendons are fibrous connective tissues that connect and transmit forces between muscle and bone. Following injury, they are very difficult to repair surgically, often resulting in tissue that is not comparable to native tendons in structural integrity and mechanical strength and are therefore prone to re-injury. A tissue engineered approach that would provide tendon tissue regeneration would be enormously valuable. A step toward this goal would be establishment of an *in vitro* system that could replicate tendon development and maturation from progenitor cells, generating tissue for transplantation capable of integrating and repairing damaged tendons. Limited progress in this area has been made to date and no system can as yet support tendon tissue maturation. In this study, I have focused on the characterisation and optimisation of a protocol using tissue engineered constructs designed to mimic tendon development, monitoring cell self-assembly and collagen deposition. Primary embryonic chick tendon cells (tenocytes) isolated at embryonic day 14 (E14), from the metatarsal tendons plated within a fibrin gel, that provides a natural substrate for the cells to self-assemble into tendon-like constructs. The cell-gel mixture was plated in between two sets of pins and suture and left in culture for up to 28- days. I show that regions of high collagen deposition are present in distinct regions within tendon constructs, centrally and peripherally. Further analysis of these regions of high collagen deposition was a focus with the goal of understanding and replicating these conditions throughout constructs. Alignment of pins in the experimental set up was important for consistent central deposition of collagen with fibres that were aligned along the long axis of the construct. While improvement of the culture system is required to produce more homogeneous tendon-like tissue, it provides an opportunity to examine the patterns of collagen deposition and uncover the conditions that best support collagen. The establishment and characterisation of these mini-tendon constructs provides an *in vitro* system to further our understanding of the self-assembly process, to work toward improving tendon-like tissue generation, as well as providing a tool for in vitro testing of molecular pathways and processes required.

Acknowledgements

First and foremost, I would like to express my thanks to my supervisors Prof Paula Murphy and Dr Rebecca Rolfe, your support, guidance, and patience throughout this project is greatly appreciated and I am extremely grateful to have had the opportunity to work alongside and learn from you both. Thank you to the other members of my lab group Lauren Sliney and Ebru Talak Bastürkmen, your kindness and help is much appreciated, I wish you both all the best.

Thank you to the postgrads, postdocs, and staff of the Trinity Zoology Department, past and present, for making the Department such a friendly and welcoming place. Particularly, to the incredible friends I have made since I have started this project, who have made the move to Dublin so easy and instantly made me feel at home. I feel very privileged to have been able to know and work alongside all of you. Thanks also to Alison Boyce and Sinead Kelly for helping us with the egg collections and support with the lab equipment.

Finally, thank you to my family, your endless support and encouragement means the world and I am so lucky and blessed to know you're always there.

Table of contents

List of Tables

List of Figures

1: Introduction

1.1 Tendon structure and physiology

The musculoskeletal system is responsible for providing structure and support to the body and allowing for movement. It is comprised of bones, muscles, joints, cartilage, ligaments and tendons (Felsenthal and Zelzer, 2017). Movement of the skeleton comes from the transmission of force from muscles to bones which is carried out by the tendons (Bobzin et al., 2021). Tendons are fibrous connective tissues that connect and transmit forces between muscle and bone to allow for and facilitate movement within the joint (Kannus, 2000, Andarawis-Puri et al., 2015). Each muscle within the body generally has two tendons, located proximally and distally. This arrangement allows for the transfer of contraction forces generated by the muscle to the bones, providing movement. The point of attachment of a tendon to a muscle is the myotendinous junction, while the osteotendinous junction is used to describe the point of attachment of a tendon to bone (Wang, 2006, Schweitzer et al., 2010, Aparecida de Aro et al., 2012). The size, shape, width, and force-transmitting properties of individual tendons within the body are largely determined by the muscles to which they are attached. Tendons attached to large muscles such as the quadriceps and triceps brachii which create large, powerful resistive forces, are short and broad making them more robust. In contrast, tendons attached to smaller muscles, such as the finger flexors needed for delicate, precise movements, are long and thin (Kannus, 2000).

Tendons display a highly organised and hierarchical structure consisting primarily of collagen fibrils arranged in densely packed bundles parallel to its long axis. It is the organisation of these collagen fibrils that gives tendons their high tensile strength (Birk et al., 1995, Kirkendall and Garrett, 1997). The most abundant form of collagen found within tendons is type 1, which makes up approximately 90% of the total collagen present within tendons (Thorpe and Screen, 2016). The remaining collagen types include, but are not limited to 3, 5 and 12. Types 3 and 5 support the deposition of collagen 1 within tendons and stabilise the tendon during development. Types 5 and 12 also play an important role within matrix organisation of the collagen 1 fibrils (Riley, 2003, Gelse, 2003). Collagen is found alongside elastin which accounts for 1-2% of the mass, both are embedded within a proteoglycan-rich matrix (Hess et al., 1989). Figure 1.1 is a diagrammatic representation of the structure of a tendon, illustrating the organisation of the collagen fibrils within the tendon tissue (adapted from (Kannus, 2000)). The collagen fibrils form larger collagen fibres (Fig 1.1 a) which are then grouped together by the endotenon, a sheath of connective tissue that binds the fibrils and fibres together (Fig 1.1 b). These form into the primary, secondary, and tertiary fiber bundles which make up the

tendon, the tendon is surrounded by a layer of thin connective tissue referred to as the epitenon, (Fig 1.1 c) which allows for smooth gliding of the tendon with adjacent tissues (Hess et al., 1989, Kannus, 2000, Birk et al., 1995).

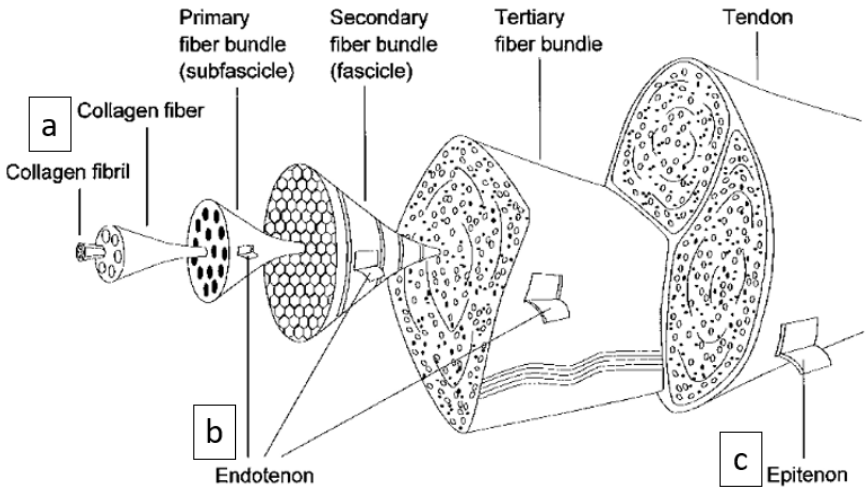

Figure 1.1. The organisation and structure of the collagen fibres and fibrils within a tendon (adapted from (Kannus, 2000)). a) Collagen fibrils group together to form larger collagen fiber bundles. b) the Endotenon a sheath of connective tissue that binds the fibrils and fibers together. c) Epitenon, a thin connective tissue surrounding the primary, secondary, and tertiary fiber bundles.

1.2 Development and maturation of tendon tissue

Tenocytes make up 90-95% of the cells in healthy tendons (Kannus, 2000). These cells form collagen fibrils that align, organise and fuse both laterally and linearly during tendon development (Birk et al., 1995). In the chick, embryonic tendons are first visualised in the limb at day 4-5, Hamburger Hamilton stage 24-24 (Hamburger and Hamilton, 1992) and are coordinated with the development of both muscle and cartilage (Kardon, 1998). Tendons arise from three sets of tendon primordia that appear in the future position of major tendons from proximal to distal (Roddy et al., 2009, Kardon, 1998). Embryonic tendons enlarge and align in the position, of each muscle attachment point over the following days. Between E16 and E18 an abrupt transition in the biomechanical maturity of the tendons occurs, whereby structural remodelling results in tissue that possesses load-bearing, structural and biomechanical properties required for tendon function (Birk et al., 1995, Mcbride et al., 1988, Peterson et al., 2021). This mechanical loading is crucial for the maturation of tendon tissue.

1.3 Tendon injury and current repair methods

Tendon injuries pose significant challenges in the field of orthopaedics and their study and classification is crucial for the development of effective prevention and treatment strategies. They can arise from a variety of conditions including overuse, increased straining of the tendon tissue, overloading, or a high speed or high impact event (Walden et al., 2017, Galloway et al., 2013). Tendon injuries occur in both healthy and compromised tendon tissue (Lui, 2015). The number of new cases worldwide each year is approximately 80-90 per 100,000 inhabitants, which equals to around 6-7 million (Bergamin et al., 2023). Tendons have a limited capacity for natural healing due to the low cellularity, hypovascularity and low metabolic activity of tendon tissue, which often results in scar tissue formation and increase risk of further injuries. Even with surgical intervention, a repaired tendon is not of comparable strength and resistance as native healthy tendons (Wang, 2006, Ruiz-Alonso et al., 2021). There are a number of ways in which tendon injuries are characterised, depending upon how the injuries arise, the length of time the patient has suffered with the injury and the extent of the damage. Tendinopathy is the broad term used to describe tendon overuse injuries that cause pain and swelling (Millar et al., 2021). Within this there are different methods in which the tendons can become injured, such as tendinitis which is caused by micro-tears within the tendon tissue due to overloading of the muscle both over time and suddenly. This causes inflammation of the tendon. Alternatively tendinosis is caused by degradation of the collagen within the tendon from overuse (Bass, 2012). These often result in ruptures and tears of the tendon tissue (Galloway et al., 2013). Damage can also occur within the paratenon which is the loose connective tissue found surrounding tendons such as the Achillies, Patella and Quadriceps and is referred to as Paratenonitis. This is inflammation believed to be caused by overuse and strain of the tendon tissue (Kvist et al., 1988). Tendon damage and injury doesn't only affect the fibres within the tendon tissue, it has been shown to also affect the biochemical environment within tendon tissue. Jelinsky et al, reported that there are significant differences in gene expression patterns between damaged and healthy tendons with a total of 983 genes found to be expressed differently within tendons suffering from tendinopathy, indicating the biomechanical environment changes after injury. Although it is unknown whether this is a cause or manifestation of the disease it is interesting to consider when investigating injuries and their causes further (Jelinsky et al., 2011).

The current treatment and repair methods for tendon injuries consist of surgical intervention. One of the most common methods of surgical repair following a tendon injury involves stitching the ruptured ends together using suture, followed by resting the tendon to

encourage regeneration and repair of the tendon tissue (Rawson et al., 2013, Chartier et al., 2021). However, this often results in partially repaired tissue that is prone to further injury, as it does not possess the same structural, functional, and biochemical properties of native tissue (Ruiz-Alonso et al., 2021).

1.4 The use of scaffolds as repair solutions

The use of engineered scaffolds to promote growth and regeneration of tissue following transplantation is a promising proposed solution for tendon healing, due to the highly organised nature of tendon tissue (Rodrigues et al., 2013). Biological or synthetic scaffolds were hypothesised to promote growth and regeneration of cells both in the laboratory and following transplantation *in vivo*. They could provide stability, support and in can be engineered to provide biological cues to both the transplanted cell populations and the endogenous cells in the damaged tissue, promoting effective reconstruction (Vasiliadis and Katakalos, 2020, Zhang et al., 2023). The main objective of the use of a scaffold is to provide a suitable environment for tissue regeneration and matrix remodelling through facilitating the attachment, proliferation, and migration of seeded cells (Walden et al., 2017). Natural-based biological scaffolds derived from mammalian tissues do not produce an immune response, and often have higher biocompatibility and biofunctionality compared to synthetic scaffolds so are often chosen as candidates for tendon regeneration and repair (Chen et al., 2009, Rodrigues et al., 2013). However, the use of biological scaffolds such as collagen for tendon regeneration have shown varied success in published studies, for example Butler et al. incorporated bone-marrow-derived mesenchymal stem cells with a collagen scaffold to repair damaged tissue in the patellar and tibial insertions in rabbits but the repair did not show complete recovery (Butler et al., 2010). This could be due to reliance on the scaffold for support, generating a cellular organisation and structure that is not found naturally, resulting in a repaired tissue that does not possess the necessary load-bearing capacity of native tendon tissue (Ruiz-Alonso et al., 2021). This indicates the need for an alternative solution to tendon regeneration and repair one that provides long-term functional repair. This must be informed by understanding further what is needed for repair and regeneration.

1.5 Organoids and their use as *in vitro* systems

Tissue engineering could provide an alternative long-term solution for tendon damage. Organoids are defined as three dimensional (3D) *in vitro* systems which represent miniaturised

and simplified model systems of organs (Hofer and Lutolf, 2021, Tang et al., 2022). They hold the potential to be used as *in vitro* systems for mechanism and pathway testing as well as determining the development of organs and tissue, alongside disease modelling and drug testing. Although the systems are simplified versions their use in this way holds great potential and promise for the field of tissue engineering due to their ability to mimic certain features of structure, function and physiology of tissues and organs (Gehwolf et al., 2019, Hofer and Lutolf, 2021). The use of these three-dimensional models compared to growing cells in two-dimensional culture includes the ability to incorporate and study cell-cell and cell-matrix interactions, as a variety of cell types can be incorporated into the models. The understanding of such interactions is critical to understand the development and maturation of tissues (Tang et al., 2022). A number of attempts have been made to produce a variety of tissues as organoids from the use of cardiac cells to create a three dimensional cardiac organoid (Cho et al., 2022), as well as the creation of tumour hybrid organoids to model drug response and tumour growth within the liver (Skardal et al., 2015).

1.6 Generating a tendon organoid.

Kadler and colleagues developed a scaffold-free self-assembly culture approach, a 'tendon organoid' which involves seeding chick embryonic tenocytes within a fibrin gel (Breidenbach et al., 2015, Kalson et al., 2011, Kalson et al., 2010, Kapacee et al., 2008, Yeung et al., 2015). This approach was shown to be able to replicate early developmental steps of cell alignment and collagen synthesis, producing parallel bundles of narrow-diameter collagen fibrils, generating a construct comparable to an immature tendon. However, to date this system has not been able to replicate the transition in later development to produce tissue comparable to neonatal tendons, nor has it been successful in attempts to repair injuries (Breidenbach et al., 2015). Yeung et al. compared performance of constructs grown in fibrin to collagen and, using a transcriptomics approach to profile the tissues, found that fibrin replicated the expression profile of embryonic tendons *in vivo* better than collagen, and encouraged better collagen production by the tenocyte cells (Yeung et al., 2015). This system provides a valuable opportunity to explore the conditions that promote better tendon-like tissue assembly, or at least appropriately prime cells to do so, not only for the eventual potential goal of engineering replacement tissue but in the shorter term, as an *in vitro* assay system to investigate and explore the signalling pathways and cues that drive transition to a more mature tendon tissue.

1.7: Aims and objectives of the project:

Late tendon development and maturation into a load-bearing tissue is one of the lesser understood components of tendon biology, which has hindered progress in providing an effective repair and tissue-engineered solution for tendon injuries. In order to begin to understand these processes further we firstly need to develop a system in which the mechanisms and pathways which are responsible for the maturation of tendons can be understood. This project aimed to characterise tendon constructs grown from embryonic chick tenocyte cells self-assembled within a fibrin gel on a cellular and molecular level.

This was achieved through the following steps:

1. Adapt and optimise the protocol published by Kadler and colleagues within the host lab for our aim of creating an *in vitro* model for investigating tendon development and maturation.

2. Characterise and analyse constructs grown from embryonic chick tenocyte cells – (initially timepoints of 7, 9, 11 days post plating, followed by 7, 14, 21 and 28 days) to determine what is happening within constructs across time, through histological and cellular analysis, focused on collagen deposition and alignment within the tendon constructs.

3. Molecularly profile gene expression in tendon constructs across time using quantitative Real Time-Polymerase Chain Reaction.

2: Materials and Methods

2.1 Primary cell culture: Fertilised Ross 308 strain chicken eggs were sourced from a commercial hatchery in Co. Kildare (supplied by Allenwood Broiler Breeders), Ireland and incubated for 14 days at 37.7°C, 5% humidity to reach Hamburger-Hamilton (HH) stage 38/39 (Hamburger and Hamilton, 1992). The hindlimbs of each embryo were dissected and the metatarsal tendon bundles (between ankle and foot) removed. Tendon bundles were then placed in filter sterilised trypsin (25 mg/ml) and collagenase (1000 U/ml) mix for 90 mins to release the tendon fibroblasts (tenocytes). The mixture was triturated every 30 mins with a smoothened (flamed) sterilised glass pipette. 3 ml of Foetal Bovine Serum (FBS) was added, and tenocyte cells were recovered by passing through a 70 µm cell strainer and centrifuged for 5 mins at 400 x g, before being resuspended in growth media, (DMEM + GlutaMAX, containing L-glutamine (2 mM), penicillin streptomycin (100 µg/mL), sodium pyruvate (1 mM), and 10% Foetal bovine serum (Gibco) before cell counting. Primary cells were plated on T75 flasks (Sarstedt); with $1.3x10^6$ in 15 ml of growth media, per T75 flask. Cells were expanded to approx. 80% confluency and passaged up to a maximum of four times (P4), until a sufficient number of cells were generated for each experiment; usually to produce 24 constructs (4 plates of six).

2.2 Plating cells for self-assembly constructs: Cells were plated for self-assembly into tendon-like constructs following the protocol described by Kapacee et al (Kapacee et al., 2008), with modifications as specified. To prepare the plates, 2 ml of SYLGARD (type 184 silicone elastomer, Dow Chemical, Midland, MI) was added to each well of a 6 well tissue culture plate and left overnight at 55°C to induce polymerisation. Once set, 2 pairs of minutiens insect pins (0.1 mm diameter, Fine Science Tools GmbH, Germany) were placed 10 mm apart in the centre of the each well using sterilised forceps. The pointed ends of the pins were pushed into the set Sylguard to ensure they remained secure and upright. A piece of silk suture (Mersilk Suture 3/8C 19MM FS-2) was secured and held in place at each end between the two pins in each set. A template was used to improve consistency between wells and plates (Figure 2.1.1). Plates were sterilised before construct seeding by placing under a UV lamp in a biological safety cabinet for 1hr, washed with 100% ethanol for 15 mins and allowed to air dry under a sterile laminar flow hood.

Primary tenocytes that had been expanded no further than P4 were collected following standard trypsinisation and resuspended at $1.6x10^6$ cells per ml. These cells were combined

with Fibrinogen (From Bovine Plasma, F8630-1G, Sigma-Aldrich, Prepared at a concentration of 20 mg/ml) and Thrombin (From Bovine Plasma, T4648-1KU, Sigma-Aldrich, Prepared at a concentration of 4 U/ml) to catalyse gelation upon plating as follows: for each well within the 6 well plate 83µl of Fibrinogen and 10 µl of Thrombin was combined with 400 µl of cells, the quantities multiplied up depending on the number of constructs being plated at one time (note: a maximum of 2-3 plates were prepared at one time to avoid premature fibrin gel formation prior to plating). 400 µl of the fibrinogen/thrombin-cell suspension was pipetted into the centre of the well, between the sets of pins and allowed to spread out covering the surface of the well but not touching the sides, a 10 µl pipette tip was sometimes used to encourage the suspension to spread out. The fibrin gel was then allowed to form and completely set in the incubator (37 °C) for 20 minutes before being flooded with 3 ml of growth medium. Every two days a sterile 10 µl pipette tip was used to gently lift the edges of the fibrin gel from the Sylgard to release points of adhesion and encourage rolling of the gel between the points of stress created by the sets of pins and suture. Rolling was the term used to describe the process during which the sides of the fibrin gel and cells meet and join to form the construct (process seen visually across time Figure 3.1.1). The medium was changed every 2 days, and the constructs were imaged and monitored every day to track rolling visually over time. At 9-, 14-, 21- and 28-days post plating, individual constructs were harvested for analysis as required. One plate of six constructs was taken for each timepoint; three constructs from each plate were prepared for histological analysis and three constructs were placed in Trizol for RNA and protein extraction. In some cases, a full plate of six constructs at each timepoint was not taken for analysis in each experimental replicate. This was due to multiple experimental factors such as constructs not developing properly i.e rips in the fibrin gel during rolling, infection, or growth of thin construct tissue that did not visually match the other constructs. Each construct grown was examined and tracked throughout its growth and for consistency and comparison. Only constructs that had fully developed and showed signs of healthy tissue were harvested and used for analysis purposes.

2.3 Construct fixation, embedding and sectioning: Constructs were fixed in 4% PFA in PBS for 30 minutes in the 6 well culture dish, washed and stored in PBS in the fridge until proceeding to wax processing. They were then washed in the following solutions: 0.85% NaCl for 30 mins at 4°C, 50% ethanol/0.85% NaCl 1:1 ratio for 15 mins at room temperature x2, 70% ethanol for 15 mins x2, 15 mins 95% ethanol. To lightly stain the constructs for visibility in wax blocks, a few drops of 0.1% Eosin (in water) was added to this last wash. For the following

steps the Sylgard base with construct attached was removed from the plate and trimmed around the construct, placed in glass dishes, ensuring that the specimen was completely submerged, and treated as follows; 20 mins 100% ethanol x3, 10 mins Histoclear II x2. The next steps were carried out in an oven at 60°C, ensuring that fresh paraffin wax (SURGIPATH-PARAPLAST) fully melts between each step. Histoclear: paraffin 1:1 ratio for 20 mins, 100% wax 20 mins x3. The specimens were placed into cassettes for wax embedding and left to set overnight on a cold plate. Wax embedded constructs were sectioned at 8 microns on a microtome (Leica, RM2255), and placed on superfrost plus microscope slides (Epredia:J1800AMNZ). Adjacent sections were placed on consecutive slides to allow for comparative analysis and by multiple staining methods. Before staining and analysis, slides were dewaxed in Histoclear II for 5 min x2, then hydrated through the following series: 100% ethanol 2 mins x2, 90% ethanol 2 mins, 70% ethanol 2 mins, H_20 2 mins.

2.4 Trichrome staining: Masson trichrome stain (Sigma-Aldrich) can be used to differentiate collagen and muscle fibres in histological samples. De-waxed sections were stained using Harris Haematoxylin solution for 10 seconds, (ref- HHs32-1l), washed in H_20 2 mins, then stained in Biebrich scarlet acid fushin 10 seconds, washed in H_20 2 mins, stained in Phototungstic/molybic acid (1:1:2H_20) solution 5 mins, and finally Analine blue for 10 seconds. Slides were then dehydrated by placing in 70% ethanol 2 mins, 90% ethanol 2 mins, 100% ethanol 2mins x2, Histoclear 5 mins x2. The slides were mounted with DPX mounting medium (Sigma Aldrich ref-1.00579.0500) and imaged using an Olympus DP72 microscope camera and Olympus CellSens imaging software.

2.5 Detection of Collagen on tissue sections using pan Collagen binding protein (CNA35): CNA35 is a bacterial pan-collagen binding protein that has been engineered to add fluorescent tags for easy detection (Aper et al., 2014) using a previously optimised protocol (Mohammadkhah et al., 2017). Specifically, to improve collagen detection, heat-mediated antigen retrieval was performed by submerging the slides in sodium citrate buffer (0.1 M, Sodium Citrate pH 6.0) at 90°C for 20 mins. After cooling to room temperature, slides were washed in PBS for 5 mins twice before blocking in 1% Bovine Serum Albumin (BSA) in TBST (which consists of 1X Tris-Buffered Saline, 0.1% Tween 20 Detergent (P9416), combined with water) for 60 mins. CNA35-GFP binding protein (Mohammadkhah et al., 2017) was prepared as a 1:50 dilution in blocking solution using, applying 200µl per slide, covered with parafilm and

placed in a sealed box at 4°C overnight. The following day, the slides were washed three times in PBS to remove free binding protein before being mounted using ProLong gold antifade reagent with DAPI (Invitrogen). Sections were then visualised using an Olympus BX40 fluorescent microscope and imaged using and Olympus DP72 microscope camera and Olympus CellSens imaging software.

2.6 Picrosirius Red Staining: adjacent series of construct sections analysed for collagen binding staining were dehydrated by placing in 70% ethanol 2 mins, 90% ethanol 2 mins, 100% ethanol 2 mins x2, Histoclear 5 mins x2. Following this they were stained with 0.2% Picrosirius red stain (50 ml 1% picric acid solution (Reagecon 1065801), 0.1g direct red (Sigma-Aldrich 365548-5G)) for 1hr, before washing with 0.5% acidified water (distilled water and acetic acid) for 10 mins, and dehydrated by placing in 70% ethanol 2 mins, 90% ethanol 2 mins, 100% ethanol 2 mins x2, Histoclear 5 mins x2. The slides were then mounted in DPX mounting medium (Sigma Aldrich 1.00579.0500) until fully set.

2.7 Measurement of pin alignment: The angle tool found in the toolbar (Figure 2.7.1) of ImageJ software was used to measure pin alignment from dish images of constructs. Day 21 constructs were chosen as from this point no further rolling occurred past this point. This observation was confirmed through visual observations from multiple experimental replicates. The alignment between the pins was measured through the angle of intersection between extended lines drawn from the pin pairs on images. Three points chosen for measuring pin alignment were kept the same for each specimen to ensure consistency and allow for comparisons between specimens, they can be seen on Figure 2.7.1 a, b, c. They indicate the attachment points of the pins to the construct and can therefore be used to indicate any inconsistencies in pin alignment and how this effects rolling of constructs. Results of measuring alignment on day 21 constructs can be seen in Table 3.3.1.

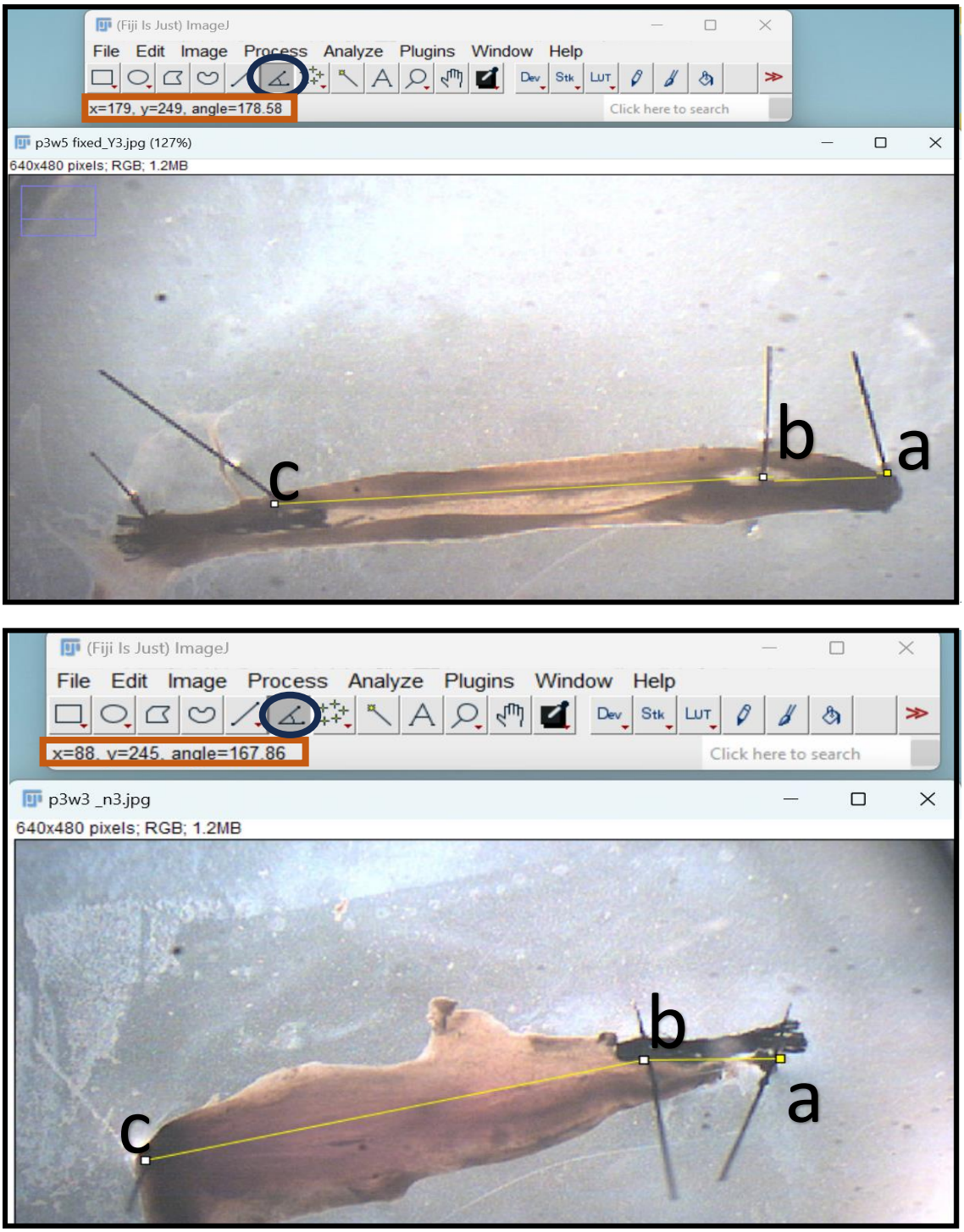

Figure 2.7.1. Approach used to measure pin alignment in 21-day tendon organoids to determine how alignment affects the ability of a construct to fully roll. The angle tool used highlighted with a blue circle. a, b, c, indicate the points at which the pins are interacting with the organoid and were used as points to measure the angle of pin alignment. Angle shown from measurement of the three points is indicated with an orange rectangle.

2.8 Directional analysis of collagen fibres using polarised light: Following Picrosirius red staining slides were imaged using an Olympus BX41 microscope, with OCULAR software installed (version 2.0.1.496). Three Regions of analysis of high collagen deposition were chosen following polarised light microscope imaging to assess the different environments of collagen deposition throughout the constructs including central and in adjacent sections to regions captured with collagen binding staining (CNA35), taken at x20 magnification. Two experimental examples were analysed for each construct analysis timepoint (9,14,21 and 28 days). Images were taken on a polarised light microscope (Olympus BX41TF Microscope fitted with polariser and analyser filters) at 45° and 0°. Following imaging, the images of both angles were merged, (Figure 3.5.1c) and six regions of interest analysed for collagen alignment were chosen, these were varying size to ensure only regions of collagen deposition without background were analysed, to make sure the completed analysis was based upon fibril orientation (example of a region of interest chosen shown Figure 3.5.1f). ImageJ software with the OrientationJ Analysis and OrientationJ Distribution Plugins were used for the analysis. Orientation can therefore be demonstrated in two ways, through the use of OrientationJ Analysis plugin which provides a colour wheel (Figure 2.5.1 e) to allow for comparative colour mapping following birefringence imaging and investigating this quantitatively using the Distribution plugin to determine the percentage of fibrils aligned within each orientation group at each analysis timepoint (Figure 3.5.2).

2.9 RNA isolation and processing from chick tenocyte cells and tissue engineered constructs: Three constructs per multiwell plate were placed in 500 µl of Trizol and placed in -70-degree freezer until required. Once ready for extraction the tissue samples were homogenised using a KIMBLE Pellet pestle motor to break up the tissue, before adding 100 µl of chloroform. Following a two-minute incubation at room temperature and 15 min centrifuge, the aqueous phase containing RNA was taken for extraction. RNA was purified using the Thermo Fisher Purelink RNA mini kit (12183018A) following manufacturer's instructions; briefly this consists of steps to bind, wash, and elute the RNA. Typically, RNA was resuspended in 30 µl of nuclease-free water and quantified using a Qubit 2.0 Quantitation System (Invitrogen) (BR RNA assay kit (Q10211). cDNA synthesis was carried out using consistently 200 ng of RNA from each individual construct and High-Capacity cDNA Reverse Transcription Kit (Applied Biosystems 4368814) and diluted 1:5 with RNase free water.

2.10 Quantitative real time reverse transcription-polymerase chain reaction (qRT-PCR) analysis: qRT-PCR analysis was used to determine relative gene expression of genes listed in Table 2.10.1. cDNA template produced from 200 ng of RNA from individual constructs was assayed in triplicate for each run, using SYBR green PCR master mix (Applied Biosystems (4309155)) and the gene specific primers listed in Table 3.8.1. Amplification was monitored on an Applied Biosystems 7500 Real time PCR system, with each run consisting of 40 cycles composed of three stages: denaturation, annealing and extension. Each sample for each gene was run in triplicate, and GAPDH was used as endogenous control gene in each case. Relative gene expression levels were calculated by subtracting the averaged Ct (cycle threshold) values of GAPDH from the averaged Ct values of each gene (ΔC^t). The difference between the Ct of the gene of interest in control groups (e.g. Embryonic day 14 (E14) in Figure 3.6.1 and P3 in Figure 3.7.1) was compared to different cell and construct timepoints, to give the relative expression ($\Delta\Delta c^t$). The relative expression of genes of interest was expressed as the fold change $2^{-(\Delta\Delta ct)}$ relative to the control group.

Table 2.10.1. Gene primer sequences used for qRT-PCR expression analysis.

Gene name	Primer sequences	Accession number
Glyceraldehyde-3-phosphate dehydrogenase (GAPDH)	FWD: 5' GGCTGAGAACGGGAAACTTG 3' REV: 5' TGGAAGATAGTGATGGCGTGC 3'	NM_204305.2
Scleraxis (Scx)	FWD: 5' CACCAACAGCGTCAACACC 3' REV: 5' CGTCTCGATCTTGGACAGC 3'	NM_204253.1
Collagen 1, alpha 1 (Col1a1)	FWD: 5' TGCTGTTGATAGCAGCGACT 3' REV: 5' GTGTCCTCGCAGATCACCTC 3'	NM_001396622.1
Collagen 3, alpha 1 (Col3a1)	FWD: 5' TTCAGGAGCAAGGGGTCCACC 3' REV: 5' AGGGAAGCTACGCCACCACCA 3'	NM_205380.3
Collagen 5, alpha 1 (Col5a1)	FWD: 5' CGACCTGGATAAAGACTTCACCG 3' REV: 5' GGCCTCCGATCCCTTCGTA 3'	NM_204790.4

2.11 Image analysis and cell quantification within mini tendon constructs: Images of defined regions of interest within CNA35: GFP and DAPI stained sections were captured at 40x magnification in appropriate fluorescent channels and were processed using ImageJ (Software: ImageJ Version 1.2.4) A typical region of interest (ROI) would include subregions of high intensity collagen detection with adjacent regions where collagen is not detectable above

background (Figure 2.11.1 b-e). ROIs were imaged and analysed for each timepoint, selecting six sub-regions of 50 µm x 60 µm for cell counts; three placed where collagen fibril detection is strong (Figure 2.11.1 b-e white boxes) and three where it is not detectable (Figure 2.11.1 b-e orange boxes). The cell counter plugin was used to count individual nuclei within each box within each ROI. This was repeated for at least four similar ROI within each construct (n=4 for days 9 and 28, n=7 for days 14 and 21).

2.12 Statistical Analysis: All statistical analysis was carried out using R studio (software version 2023.12.1 build 402), to determine the significance of data. Generally, the data produced showed normal distribution throughout. A total of 7 construct experiments were analysed across the techniques and assays shown. P values for all tests are indicated as follows *p ≤ 0.05, **p ≤ 0.01 ***p ≤ 0.001. ROI were selected from data images taken on the microscope; the number of ROI varied based upon the assay used during analysis. For example, when focusing on Collagen fibre alignment (Figure 3.4.2), total regions analysed for each graph n=6 for day 9, n=5 for day 14, n=5 for day 21 and n=6 for day 28. These regions were taken from two experimental examples (taken at x20 magnification) and were various sizes depending on the extent of high collagen deposition. An un-paired t-test was used to determine differences for collagen alignment. Graphs show the average of each alignment value with the standard error of the mean used for error bars. Relative expression data was analysed for n=5 experiments with each sample ran in triplicate for analysis of expression of cells over time in culture (Figure 3.6.1). Relative expression for tenocyte cells across time in culture was analysed for n=4 experiments with each sample run in triplicate (Figure 3.7.1). The difference between the Ct of the control groups and samples gave the relative expression ($\Delta\Delta C^t$). The relative expression of genes of interest was expressed as the fold change relative to the control embryos ($2^{-\Delta\Delta Ct}$). Statistical tests were carried out on the relative expression data to determine the differences. The explanatory variable was gene expression which was continuous, while the explanatory variable was 'gene group' which was a factored variable. The data displayed in Figure 3.6.1 showing expression in cells over time, A one-way-ANOVA was initially carried out followed by a Tukey post-hoc test. However, a Generalised Linear Model (GLM) was chosen to observe any differences between groups of cell expression. A Generalised Linear Model (GLM) was carried out using a Gaussian distribution due to the normal distribution of all gene expressions (*Scleraxis, Collagen 1, alpha 1*). Analysis of deviance with a Chi-Squared analysis of deviance was then used to investigate the relationships between groups for independence and from this p-values were extracted. For examination of

specific differences in expression between gene groups a pairwise test was created using the "emmeans" package in R studio. For the relative expression data for tenocyte cells across time in culture (Figure 3.7.1), a One-way ANOVA indicated no differences in expression across time in culture so no further statical tests were used on this data (p-values larger than 0.05).

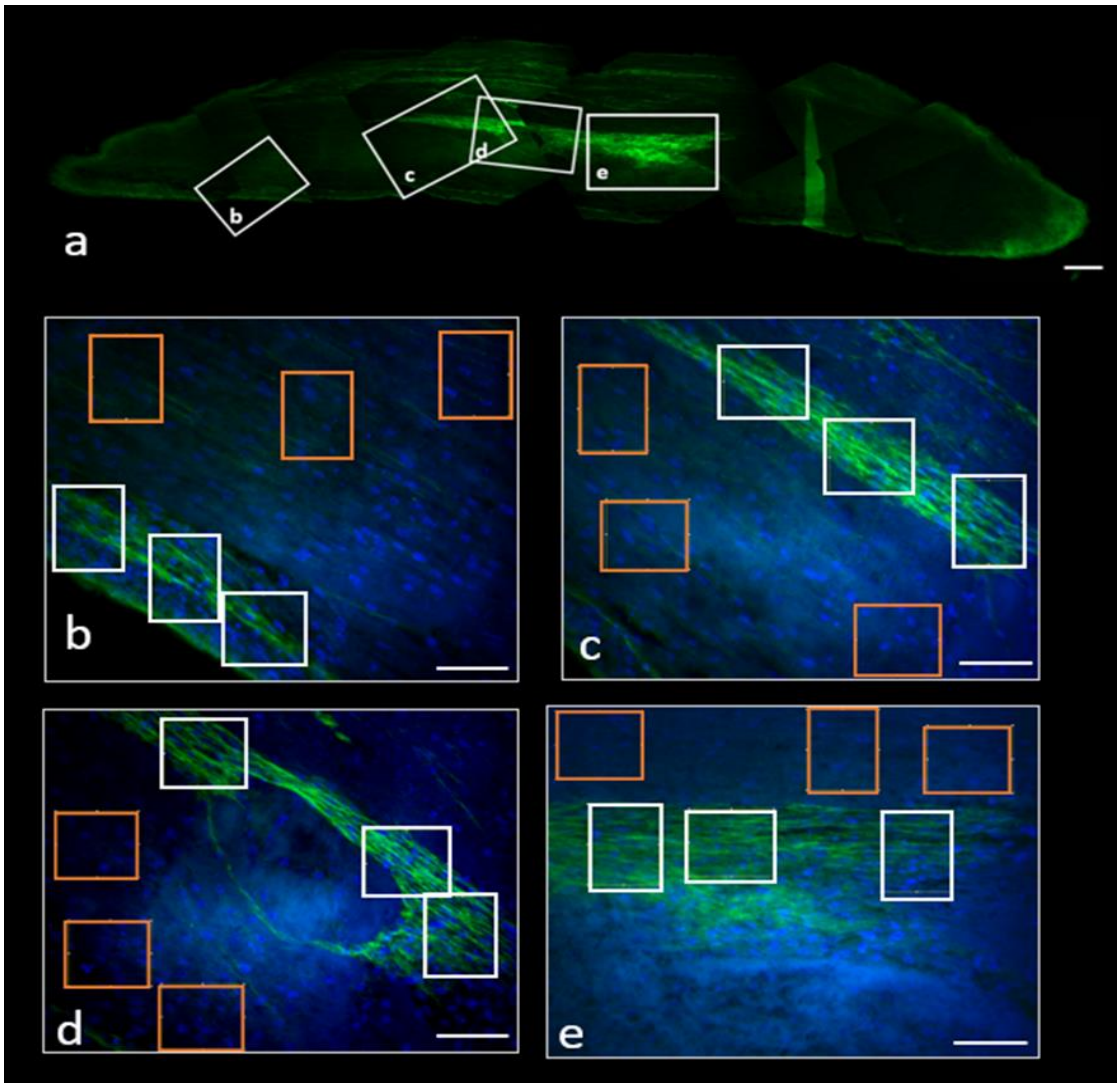

Figure 2.11.1. Cell count analysis approach to compare regions of high and low collagen deposition within defined regions of interest within *in vitro* tendon constructs. a) Tiled images of a midline longitudinal section through a day 14 construct stained with collagen binding protein (CNA35-GFP), showing regions of high and low collagen deposition in a single construct. Regions of Interest (ROIs) (examples boxed) were defined to include sub-regions of high collagen deposition adjacent to regions of low collagen deposition. b-e) show higher magnification of the ROIs in a, as merged images (CNA35-GFP in green and DAPI (cell nuclei) in blue). Within these four regions (b-e), sub-territories of consistent size (50µmx60µm) were selected, including three regions of high collagen deposition (white boxes) and three regions of low collagen deposition (orange boxes). Cell nuclei within each box were counted using the cell counter plugin on ImageJ and averaged per region of interest, in each category. Scale bars for all images are 50 µm.

3: Results

3.1 Tenocyte cells self-assemble within a fibrin gel to produce a 'mini-tendon' construct.

A total of 24 experiments were carried out to generate the 'mini-tendon' constructs using primary E14 chick tenocytes during the project. After optimising and testing the protocol for use within the lab and being able to produce constructs that self-assembled within the fibrin gel consistently in culture. Seven experiments consisting of a total of 138 constructs were generated for analysis, conditions and timelines were kept consistent between these experiments to allow for and facilitate comparison of the generated constructs. These constructs were plated at a cell density of $6.4x10^5$ cells per well and one plate from each experiment was taken for analysis following 9,14,21 and 28 days in culture. Images were taken daily of the constructs over time to assess the rate and extent of rolling. Figure 3.1.1 (a-d) shows images of 4 independent constructs from 4 experiments and the progression of their time in culture. Fibrin gel rolling generally commenced by day 3 and was in most cases completed by days 9-11 (Figure 3.1.1). There was some variability in the extent of rolling i.e the extent to which the cell/fibrin gel achieved full rolling with the sides meeting at the midline, with no visible gap (e.g. Figure 3.1.1 a, b and c) compared to incomplete rolling, with a gap between the two sides (e.g. Figure 2 d). There was variation in the extent of rolling both between replicates within the same experiment and across experiments, which is why days post plating was chosen as an analysis point. A test was carried out to determine the role of tenocyte cells in the self-assembly process (Figure 3.1.1 e)., showing that without the inclusion of tenocyte cells the fibrin does not self-assemble, indicating that it is the tenocyte cells that are driving this process.

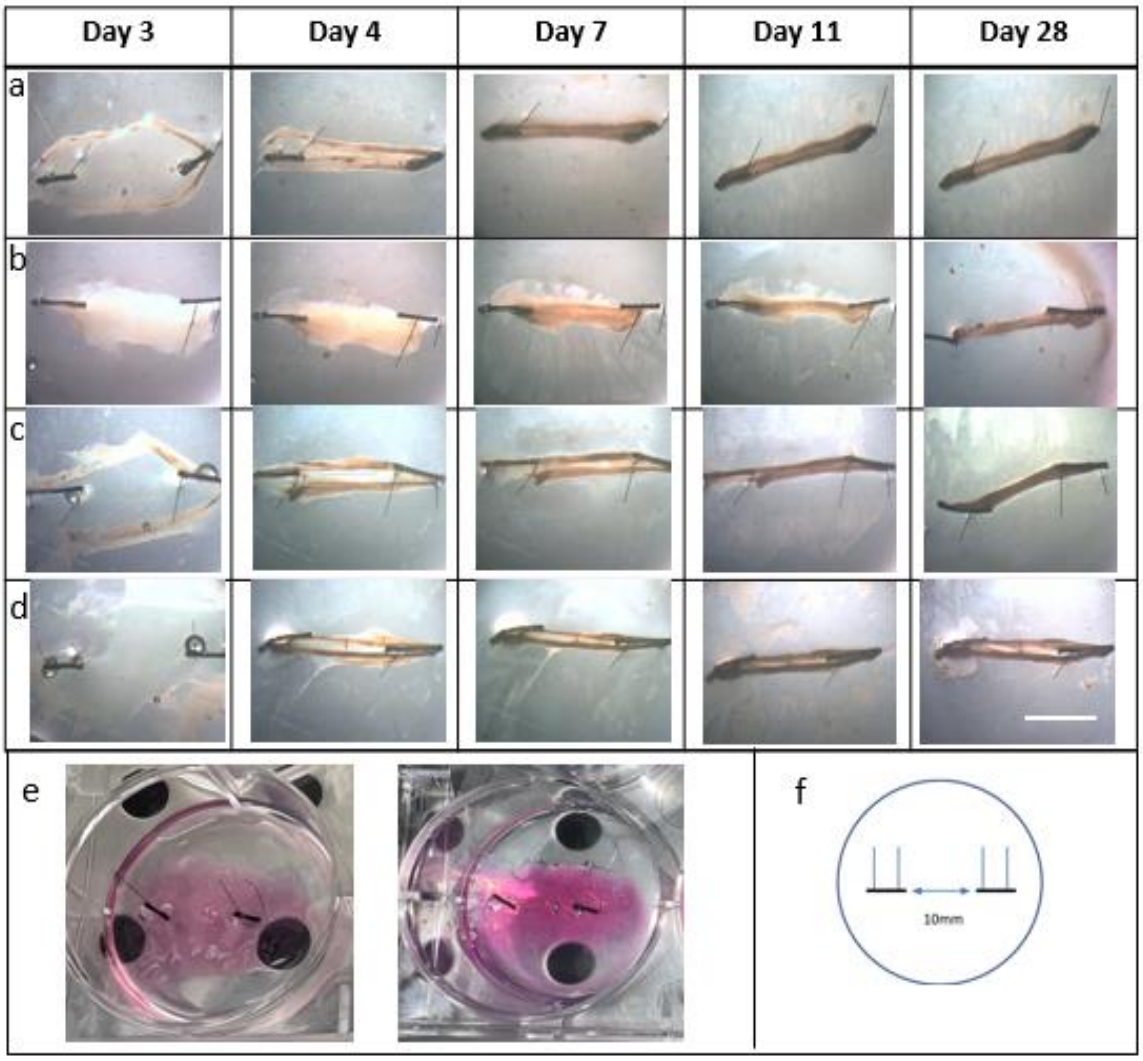

Figure 3.1.1 Representative images of four constructs showing self-assembly of mini tendons generated from primary embryonic tendon cells over time. Rows (a-d) four separate construct examples (each plated at $6.4x10^5$ cells per construct) imaged across time (day's 3, 4, 7, 11 and 28 shown), typical of the overall morphology achieved across experiments and showing the level of consistency. Note that constructs shown in a, b and c achieved complete rolling whereas construct in row d did not. Scale bar 10mm serves for all images (a-d). e) shows the results of a fibrin-test completed to demonstrate the role of tenocyte cells in the self-assembly process; the well was plated with fibrin only and incubated as normal without tenocyte cells, dish images shown are 4- and 7-days post plating. f) schematic template used when placing the pins and suture within each well of a six well dish to ensure consistent positioning.

3.2 Localised Collagen deposition is present within the 'mini-tendon' constructs.

Trichrome staining of longitudinal sections through each construct allowed crude level visualisation of the distribution of cells within the construct and an indication of collagen deposition (Figure 3.2.1). It is clear that the constructs are generally filled with cells (purple stained nuclei; Figure 3.2.1 g blue arrow) but there is not an even distribution throughout the construct. Trichrome staining highlights collagen in tendons, as seen in the image of the E14

developing tendon (Figure 3.2.1 e/f). Trichrome staining of the constructs showed some localised regions of purple staining, but collagen deposition was not easy to assess at this level. Figure 3.2.1 g and h show adjacent sections from the same construct stained with trichrome and fluorescently tagged collagen binding protein (CNA35:GFP) which more definitively shows localised seams of collagen deposition within the construct.

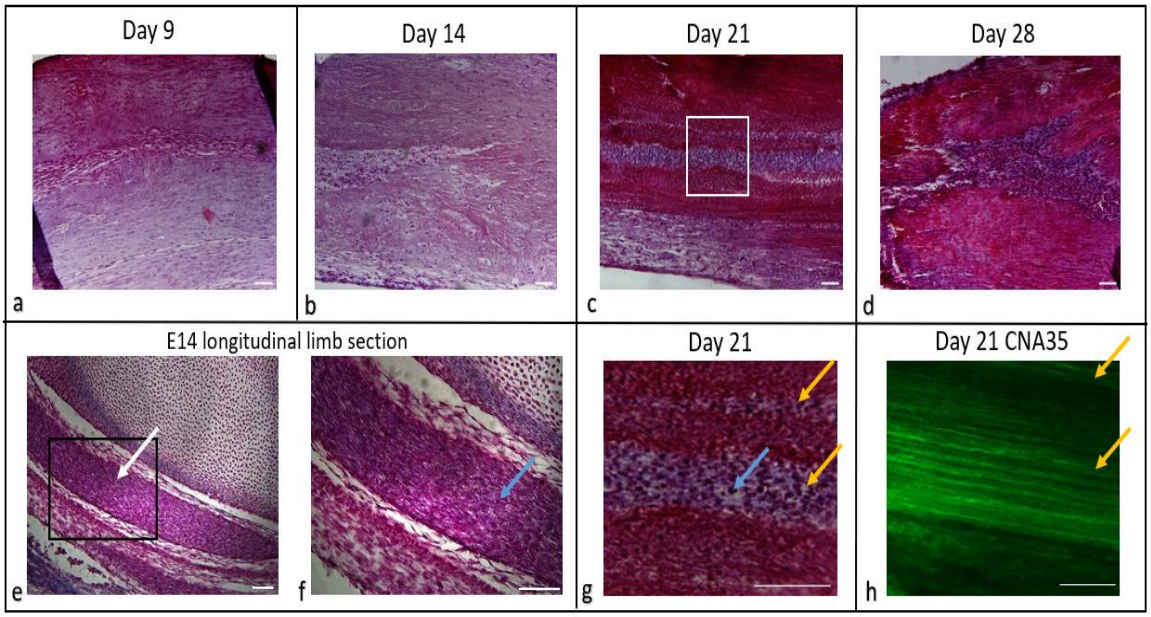

Figure 3.2.1 Masson's Trichrome staining reveals overall cellular distribution and is indicative of collagen deposition within tissue engineered constructs. a-d) Representative histological midline longitudinal sections stained with Masons' trichrome across days in culture, as indicated. e and f) a section through an E14 embryo showing the staining of a native tendon, with f showing a higher magnification of the boxed region in e, white arrow indicating tendon and blue arrow indicating a nucleus. g and h) show higher magnification views of the boxed region in c, on adjacent sections of the same construct; g stained with trichrome and h with fluorescently tagged collagen binding protein (CNA35:GFP). Blue arrows indicate a nucleus shown as dark purple staining and yellow arrows indicating regions of high collagen deposition seen as a blue/purple seam in g and bright green fluorescence in h. All scale bars shown indicate 50 µm.

Tiled images of midline longitudinal sections through each construct can be visualised to assess the overall make up and level of consistency achieved between constructs at a histological level. To examine collagen deposition throughout individual constructs, the CNA35-GFP binding protein was utilised (Mohammadkhah et al., 2017, Aper et al., 2014) together with visualisation of the nuclei using DAPI. Figure 3.2.2 a shows trichrome staining and b) the adjacent section stained with CNA35 to definitively reveal collagen deposition in a 14-day construct (Figure 3.2.2 b). Two distinct regions of high deposition were clear across all

constructs; 1) intense localised accumulation in seams that run along the long axis of the construct so, between the anchoring pins and sutures in the growing construct (white arrow in Figure 3.2.2 b), and 2) often the peripheral margins of the construct (blue arrow in Fig 4.2 b), although these regions of high collagen deposition at the peripheral are often less intensely stained than the central regions (Figure 2.4.2 b). Higher magnification views of the boxed regions in different channels show cell nuclei (DAPI; blue) and deposited collagen (green), with channels merged in the third image. This allows visualisation of cellular arrangement together with regions of collagen deposition. The collagen organisation within the construct shows clear regions of intense deposition (Figure 3.2.2 b) that are not visible with Masson's trichrome stain (Figure 3.2.2 a).

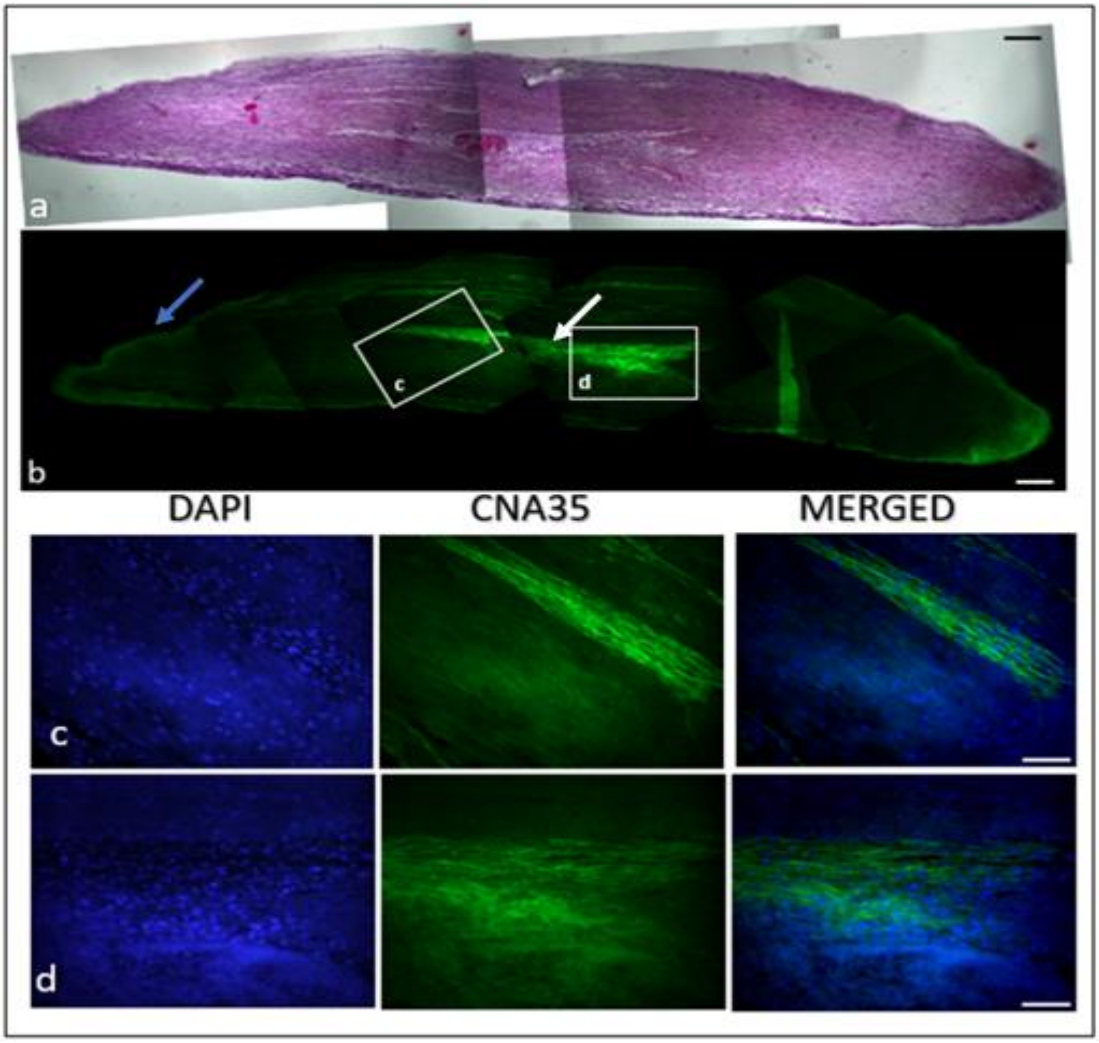

Figure 3.2.2. Regions of high and low collagen deposition are dispersed within *in vitro* tendon constructs. Pan Collagen Binding protein CNA35-GFP indicates collagen fibril accumulation within a day 14 self-assembled tendon construct. Scale bars for images a-b are 100µm are c-d are 50µm. a) Tiled images of a midline longitudinal section through a day 14 construct stained with Masons' Trichrome. b) Tiled images of an adjacent midline longitudinal section to that shown in a, stained with collagen binding protein (CNA35-GFP), showing the pattern of regions of high and low collagen deposition in a single construct. White arrow indicating regions of high collagen within the central portion of the construct and blue arrow indicating regions of high collagen deposition in the outer peripheral region. c&d) magnified views of the regions of high collagen deposition boxed in b. Images show visualisation of cell nuclei in blue following DAPI staining, and regions of collagen deposition shown in green following pan collagen binding protein. The green and blue channels are then merged so that collagen and nuclei are visualised together.

Figure 3.2.3 shows midline tiled images of constructs across different times points in culture (d) 14, a; d21, b; d28, c) from the same experiment to give an indication of the patterns and variations within regions of high and low collagen deposition within constructs across time. Through observing the constructs that have been analysed to date, collagen deposition appears not to increase over time based on observations of the overall number of localised

regions present and fluorescence intensity, seen following CNA35 staining. However, all timepoints do consistently show regions of high collagen deposition present in central and peripheral regions throughout the constructs (Figure 2.2.3). These regions of high collagen deposition which are located centrally, running along or parallel to the long axis of the construct; a line running between the two sets of pins and sutures that anchor the construct at each end. In several constructs the collagen deposition is located at the core of the construct. Figure 3.2.4 shows examples of collagen deposition in independent constructs, across different experiments, all taken at a timepoint of 21 days. We can continue to observe the pattern of linear collagen deposition, raising the question that there might be consistent localised conditions present within these central regions, both across timepoints and within experimental examples that result in high collagen deposition. Figure 3.2.4 c1 displays a construct that has not fully rolled. The region is visualised within the tiled image of the construct as a clear seam of high collagen deposition through the centre. Interestingly Figure 3.2.4 a1 shows a construct that has not fully rolled and does not appear to show a central seam of collagen deposition (although there are tears along the central line). Given the common pattern of collagen deposition at the centre of the construct running between the original position of the pins and suture support structures that create a line of tension for the construct, I speculate that the increased collagen deposition in this location is stimulated by the localised tension.

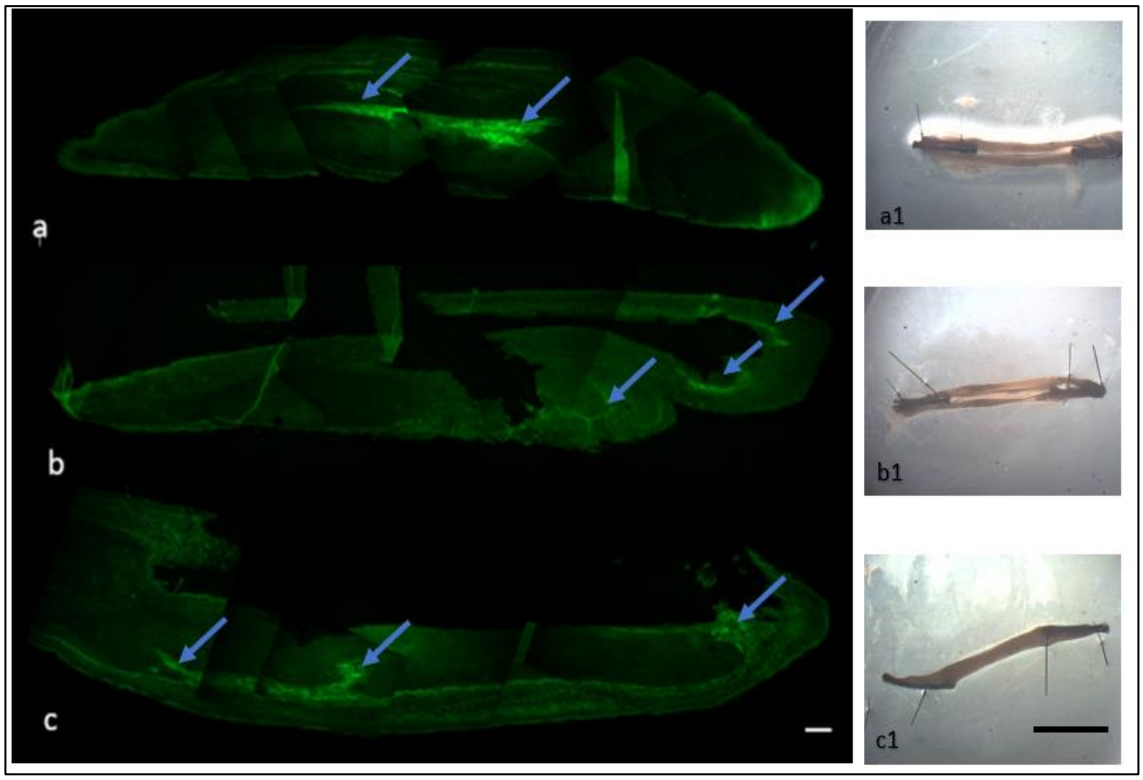

Figure 3.2.3 Collagen binding protein (CNA35-GFP) staining indicates regions of high and low collagen deposition across time in culture. a-c) are midline tiled images of mini tendon constructs at timepoints of 14, 21 and 28 days of culture from one experiment stained with pan collagen binding protein (CNA35-GFP). Scale bar 50 µm for all tiled constructs, 10mm for dish images. Blue arrows indicate regions of high collagen. In a) collagen deposition is seen at the core of the construct, whereas in b) and c), collagen deposition is more peripheral. a1, b1, c1) are corresponding dish images to tiled images a, b, c indicating if the construct fully rolled in culture. c1) is representative of a construct that has fully rolled, whereas a1, b1) are not fully rolled.

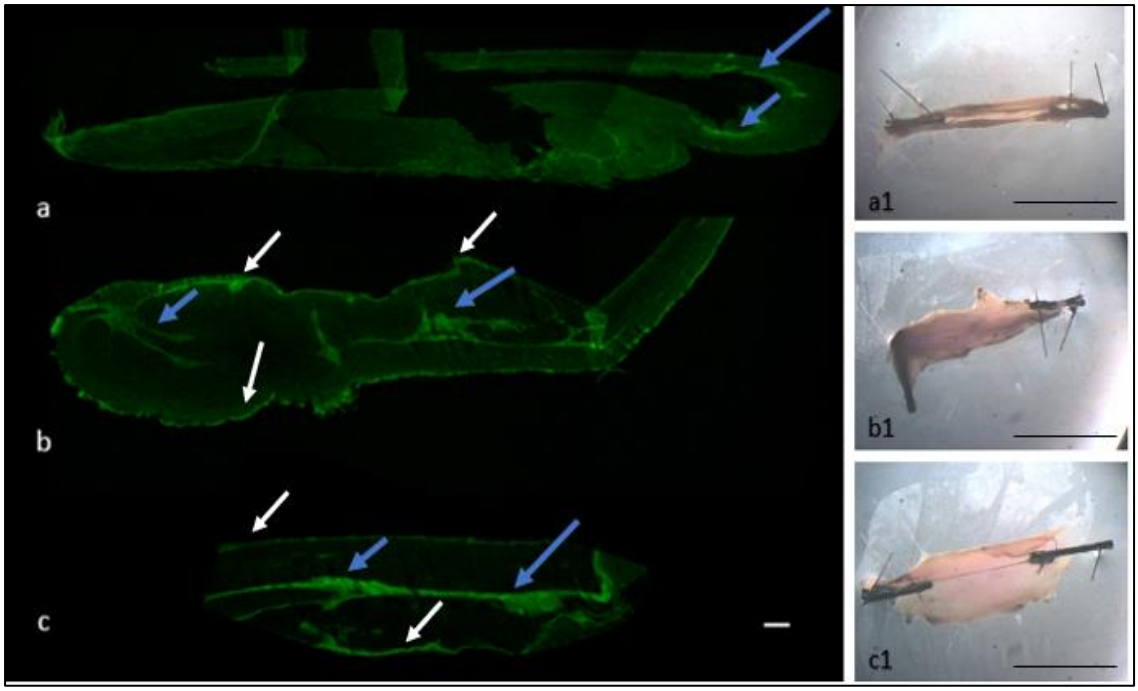

Figure 3.2.4 Examples of independent constructs at the same time point; following 21 days in culture. a-c) are different experimental examples of midline tiled images of 21-day tendon constructs stained with pan collagen binding protein (CNA35-GFP) to indicate patterns and variation in collagen distribution across experimental examples of the same timepoint. Scale bars shown are 50µm for all tiled constructs, 10mm for dish images. Blue arrows indicate regions of high collagen deposition a) represents more peripheral collagen deposition whereas b and c indicate more central seams of high collagen although both also show peripherally located collagen (white arrows). a1, b1, c1) are corresponding dish images to tiled images a, b, c) indicating if the construct fully rolled in culture and indicative of present lines of tension, a, b and c represent constructs that have not fully rolled.

3.3 Alignment of pins is an important factor in full rolling of the construct and generation of the conditions needed for collagen deposition.

Given that complete rolling is important for generating the conditions for central collagen deposition (Figure 3.4) and since there was a photo record of every construct across each day, I wished to evaluate what factors might contribute to incomplete rolling. Through observation of these dish images, it was clear there were two main sources of variation in the setup of the wells that did not remain completely consistent throughout experiments. One being the detachment of the suture from a pin during culture, (Figure 3.2.4 b1) and another being non-parallel alignment of pins (Figure 3.2.4 c1) these factors appear to cause incomplete rolling and create a disturbed line of stress.

When comparing the tiled images of constructs with their corresponding dish images (Figure 3.2.4), factors that visually appear to have affected rolling within the constructs can be observed. The alignment between the pins was measured through the angle of intersection between extended lines drawn from the pin pairs on images (Figure 2.7.1). Angles measured for these constructs are as follows Figure 3.2.4 a1) 178.56°. This image displays slight suture displacement which is affecting the constructs' ability to fully roll. Figure 3.2.4 b1) has a pin alignment angle of 167.86°and indicates a construct where the suture has almost fully dislodged on one side meaning that the construct has not self-assembled in the way in which we would expect, the surface area of the construct within the well is quite large which could be what is disrupted the central region of collagen deposition (Figure 3.2.4 b blue arrows). Figure 3.2.4 c has a pin alignment angle of 172.16°. Observing regions of high collagen deposition is particularly interesting in this case as although the construct has not fully rolled there is a central seam which appears to also be visible as a thin tension line located between the two pins shown in c1. In order to assess these factors further angles were measured for day 21 constructs across 7 experiments results shown in Table 4.3.1, complete construct rolling was noted (y/n) and suture displacement indicated with an asterisk (column 5). Notably, in every case where a suture was displaced (15), complete rolling was not achieved. The remaining 5 of the constructs where incomplete rolling did not occur the angle of intersection was particularly reduced (mean 163.1^{o} and standard error of ±4.03°) compared to cases of complete rolling (mean 172.9° and standard error of ±1.3^{o} across 15 constructs) plotted in Figure 3.3.1. The remaining 41% of 34 constructs photographed at 21 days of culture showed complete rolling. There was a difference between the angles of pin alignment measured between complete and incomplete rolled constructs, showing the importance of pin alignment on complete construct rolling (unpaired t-test, $_{(1,5)}$, p 0.03).

Table 3.3.1: Assessment of pin alignment and suture displacement on the mini-tendon constructs ability to fully roll, with angles of pin alignment shown for constructs following 21 days in culture across 7 experiments.

Experiment number	Timepoint at which constructs were taken for analysis	Number of Constructs formed from each plate	Construct fully rolled within plate (y/n)	Alignment of pairs of pins (angle of intersection in degrees) * Indicates suture displacement in at least one of the pin pairs
17	14 days	6		
	21 days	4	N	172.46
			N	162.64*
			N	154.99*
			N	148.28
	28 days	4		
18	9 days	6		
	14 days	6		
	21 days	5	Y	178.26
			Y	178.15
			Y	172.45
			N	176.37 *
			N	167.23
	28 days	5		
20	9 days	6		
	14 days	6		
	21 days	4	N	163.81*
			N	170.26*
			N	165.46*
			N	171.62*
	28 days	3		
21	14 days	6		
	21 days	6	Y	170.21
			Y	164.53
			N	177.42*
			N	170.44 *
			N	175.12 *
			N	170.21*
	28 days	5		
22	9 days	6		
	14 days	6		
	21 days	5	Y	174.01
			Y	173.34
			Y	177.04
			Y	172.67
			N	176.74*
	28 days	6		
23	14 days	6		
	21 days	5	Y	174.38
			Y	171.20
			Y	161.84
			N	163.55
			N	163.87
	35 days	5		
24	9 days	6		
	14 days	6		
	21 days	5	Y	178.35
			Y	175.56
			N	172.58 *
			N	177.61 *
			N	171.96 *
	28 days	6		

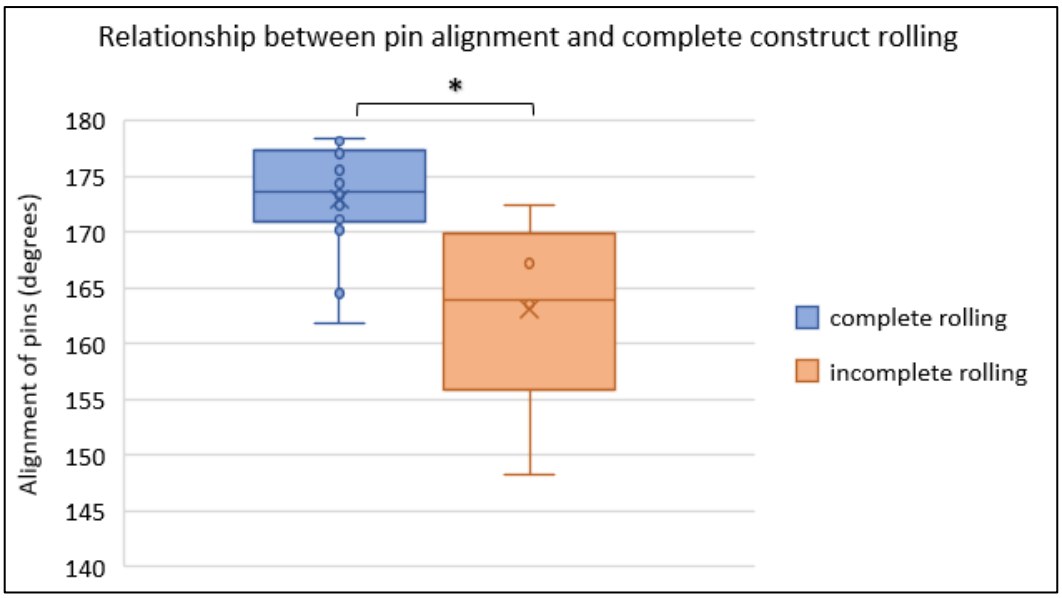

Figure 3.3.1 Alignment of pins results in more consistent fully rolled constructs. Relationship between degree of pin alignment and full rolling of constructs in 21-day constructs, showing in cases of unaligned pins complete rolling was less likely to occur even after 21 days in culture. (n=14 constructs complete rolling, n=5 constructs incomplete rolling. note: instances of suture displacement were excluded from incomplete rolling). Unpaired t-test used to determine significance between groups (*$p \leq 0.05$).

3.4 Collagen fibres are aligned along the long axis of the construct.

The relationship between alignment and collagen fibrils present in regions of high collagen deposition within the tendon constructs can be investigated through Birefringence. Collagen is a birefringent protein due to its highly organised structure, and therefore when imaged under polarised light following picrosirius red staining (Figure 3.4.1 b) the directionality of collagen fibres and be viewed and quantified. Figure 3.4.1 shows a representative region of high collagen deposition located centrally within a day 14 tendon construct and the analysis process carried out to determine the orientation of collagen fibres within. The orientation colour map (Figure 3.4.1 e), indicates that the majority of collagen fibres located within this representative region of high collagen deposition are orientated close to 90° due to the blue/cyan colour following analysis (Figure 3.4.1 d). The histogram (Figure 3.4.1 g), shows the proportion of fibres aligned within each degree, the majority of collagen fibres aligned close to 0° demonstrating this consistent orientation throughout. It is thought that perhaps a central line of tension is created throughout the construct from complete pin alignment, and it is this that is believed to cause this alignment of collagen fibres along the long axis of the construct, meaning they are all parallel to each other and in the same direction. In order to investigate

this further different regions of high collagen deposition were investigated for their collagen fibre orientation; these regions were defined as central or peripheral within the construct. Central was defined as located in the core of the construct as indicated by the white arrow in Figure 3.2.2 b, and peripheral regions defined as the collagen surrounding the edge of the construct, as indicated by the blue arrow in Figure 3.2.2 b.

Analysis of fibre orientation is shown in the box plots in Figure 3.4.2, for the two spatial sub-regions of constructs analysed, 1) central regions of constructs with high collagen deposition (representative example shown in Figure 2.2.2 b (white arrow)) (Figure 2.5.2 a), and 2) peripheral regions of constructs with high collagen deposition (representative example shown in Figure 2.2.2b (blue arrow)) (Figure 2.5.2 b). These regions were analysed across time in culture. The proportion of fibres within three orientation groupings with respect to the construct long axis: +/- 0° - 10°, +/-10° - 20°, +/- 20° - 30° are shown. There are no statistical differences within each grouping (+/- 0° - 10°, +/-10° - 20°, +/- 20° - 30°) across culture time in either of the central (Figure 3.4.2a) or peripheral (Figure 3.4.2b) regions, however, there are differences between central and peripheral collagen alignment for each time point analysed. For example, central collagen fibres in day 14 constructs show 80-62% of their fibres within the 0+/-10-degree orientation grouping compared to 55-59% of their fibres within the same grouping in the peripheral region of the construct (Figure 3.5.2 b). These finding demonstrate that collagen fibres are more aligned within central regions of constructs, suggesting that perhaps the central line of tension created by the pins contributes to creating more aligned fibres.

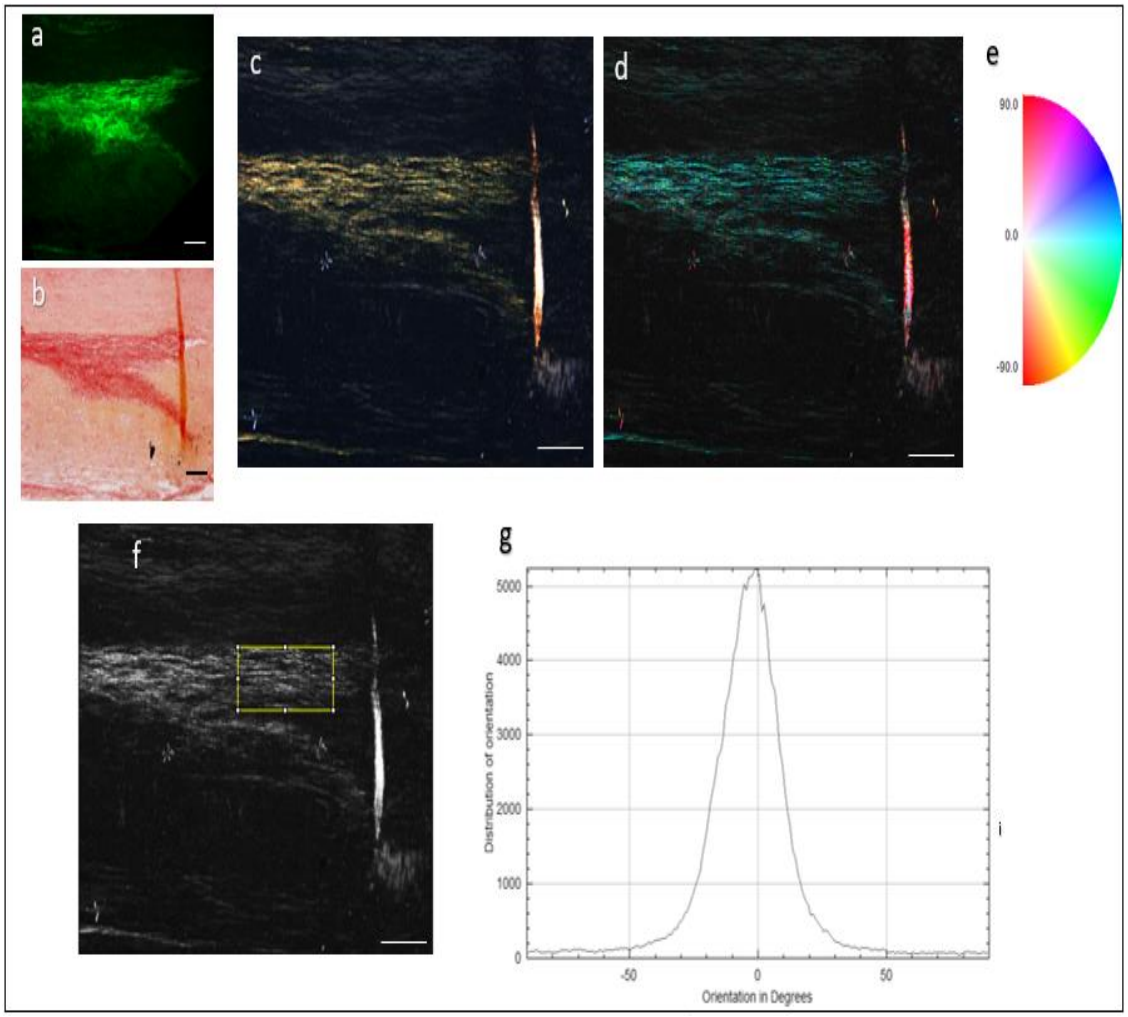

Figure 3.4.1 Collagen fibrils within tendon constructs are aligned across the long axis
Representative regions from a day 14 construct (a-f) to demonstrate the analysis process. a) shows a region of a high collagen deposition (shown in green) stained with collagen binding protein (CNA35). b) shows an adjacent region stained with picrosirius red staining. c) shows the region stained in b imaged using a polarised light microscope to assess birefringence. d) shows the image taken in c after ImageJ orientation analysis to determine the orientation of collagen fibres. e) shows the fibre orientation colour map, where blue/cyan indicates fibres oriented close to 0° and pink/red indicates fibres oriented ~90^{o} f) indicates a region of interest chosen for percentage directionality analysis. g) uses the colour map information to generate a histogram of local angles representing the mean and standard deviation of orientations for a ROI. All scale bars shown are 50 µm.

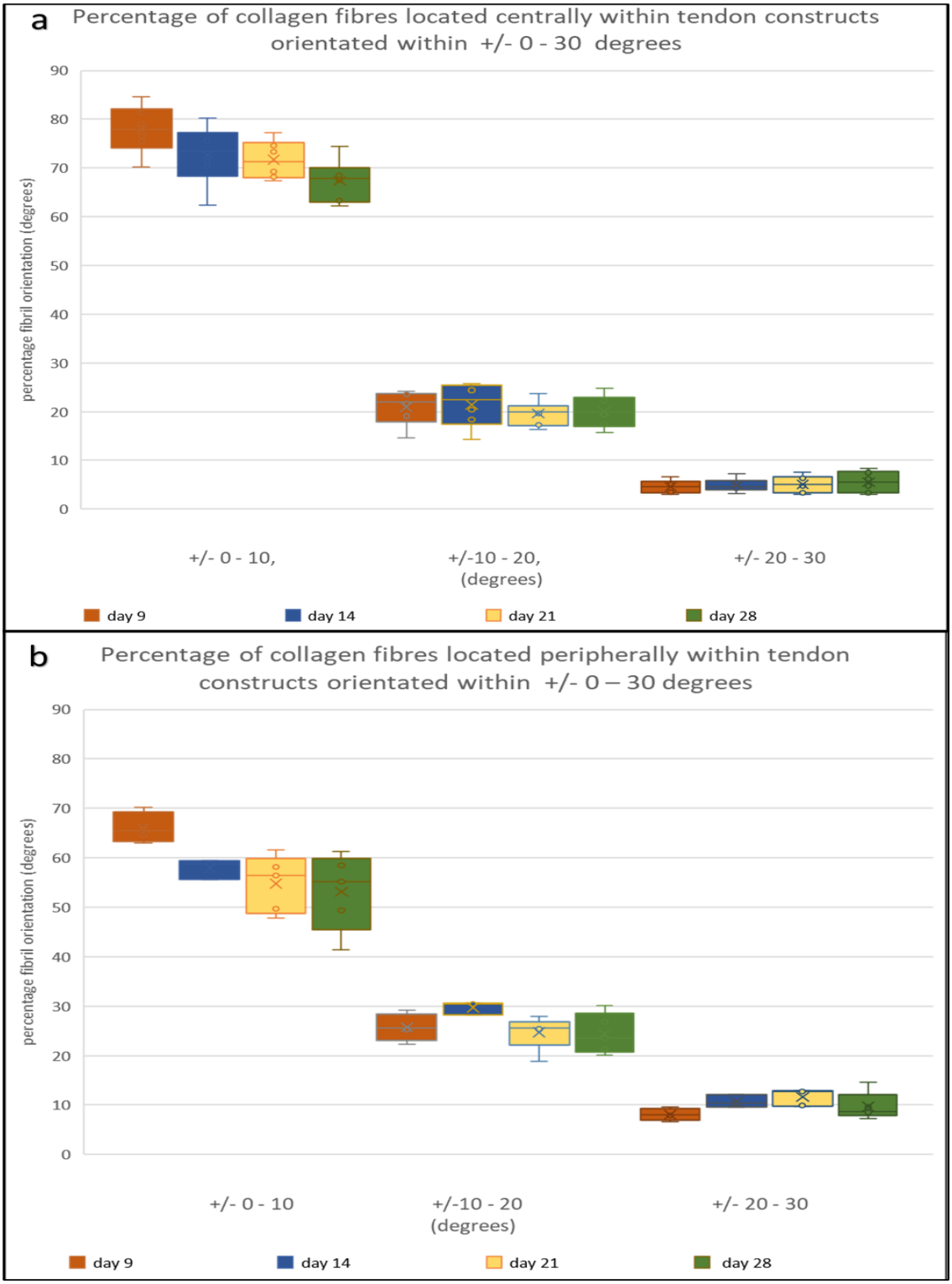

Figure 3.4.2. Collagen fibres are more aligned in central regions of mini-tendons constructs, corresponding to regions of high collagen deposition. The box plots represent the proportion of fibres within three orientation groupings with respect to the tendon long axis: +/- 0° - 10°, +/-10° - 20°, +/- 20° - 30° (ROIs measured for each high collagen environment n=12 (d9), n=10 (d14), n=10 (d21) and n=12 (d28), across two experimental examples). a) collagen alignment analysis for regions of high collagen deposition located centrally within tendon constructs b) collagen alignment analysis for peripheral regions of high collagen deposition located on the outer edges of the constructs.

3.5 Cell density is greater in regions of high collagen deposition compared to adjacent regions of low collagen deposition.

To address why localised regions, yield successful collagen deposition while adjacent regions do not, we examined cell density in adjacent high and low collagen regions as a potential reason. Sites for analysis were chosen with adjacent areas of high and low collagen deposition across all culture timepoints (days 9, 14, 21 and 28) (Figure 2.11.1). Within these sites for analysis six Regions of Interest (ROIs), were defined for cell counts (50 x 60 µm), three quadrants with high collagen and three quadrants with low collagen and compared across ROIs. Figure 3.5.1 shows that there were significantly higher numbers of cells per area in regions of high collagen deposition consistently across all timepoints when compared to adjacent regions of low collagen deposition. Comparing the counts for high collagen areas against each other per day of culture, and similarly the counts for low level collagen areas against each other across time in culture also show that there is no significant change in cell number across time in culture within these defined regions.

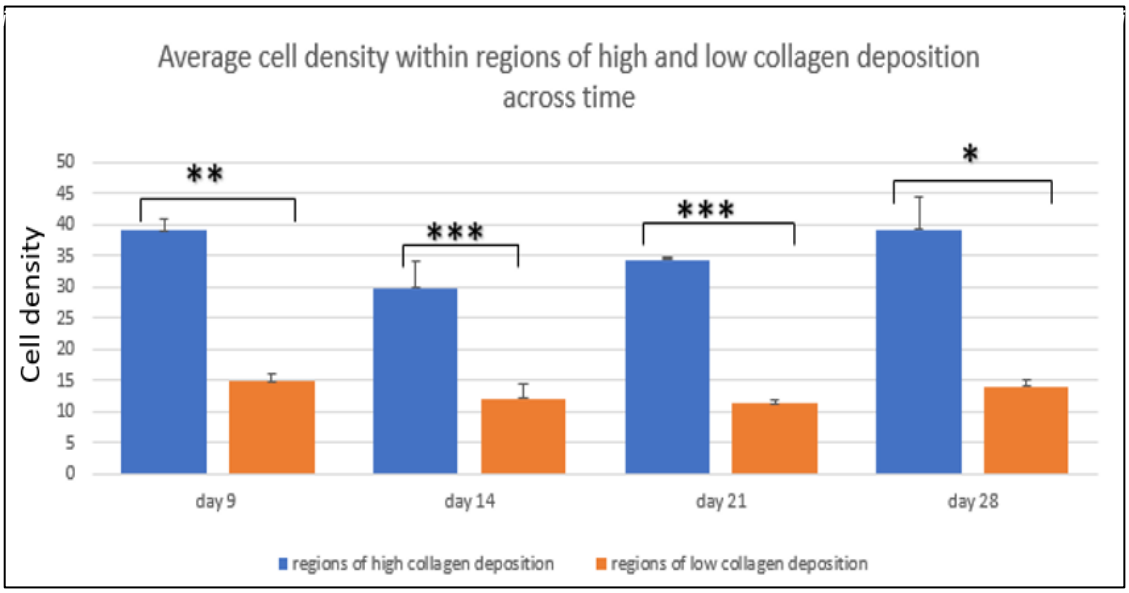

Figure 3.5.1 Cell density is greater in regions of high collagen deposition compared to regions of low collagen deposition. Cell counts across regions of interest were compared for high and low collagen territories. Total independent regions of interest imaged for each time point n=4 - days 9 and 28, n=7 - days 14 and 21, over a total of three experimental replicates. Significance between the mean cell counts within regions of high collagen deposition and low collagen deposition indicated (*p ≤ 0.05, **p ≤ 0.01 ***p ≤ 0.001). No difference was found among pairwise comparisons of high and low cell counts of the same culture day (pairs of blue and orange data sets)

3.6 Collagen 1 and Scleraxis are continually expressed in tenocyte cells.

To monitor the molecular profile of primary cells following culture, qRT-PCR analysis of tendon marker genes and collagen genes was assayed and compared between native tendons from E14 embryos (the tissue from which the cells are derived), cells newly extracted from the tendons prior to plating (primary cells) and following different numbers of passages (P) in monolayer culture (P1 to P3) before self-assembly into constructs. Relative expression was calculated as described in (3.9) and normalised to E14 GAPDH expression. To examine the stability of tendon gene expression in cells, prior to plating in constructs, Scleraxis (*Scx*) and Collagen 1, alpha 1 (*col1a1*) expression was analysed. This was done first within E14 tenocytes to P1 cells to show changes from initial removal from the embryo to initial plating on plastic (Figure 3.6.1 a, c). Relative expression was then analysed from primary cells (following treatment of the tendon bundles with enzyme to release tenocyte cells) to plated passages that were used to increase cell number for the generation of constructs (Figure 3.6.1 c, d). The relative expression for *Scx* within tenocyte cells across time in culture shows a decrease in expression from initial removal from the embryo (both E14 and primary cells) to plating on plastic (p1 cells) (Figure 3.6.1 a) (GLM, analysis of deviance $x^2_{(2,12)}$ $p < 0.005$). Within the groups, the e14 and p1 were different (emmean, t(12) = 4.206, $p = 0.003$), and p1 and primary were different (emmean, t(12) = -4.03, $p = 0.0044$). The relative expression across passages p1 -p3 (Figure 3.6.1 b) shows *scleraxis* is continually expressed across its time in culture. However, the level of expression decreased from the embryo to culture. (GLM, analysis of deviance $x2_{(3,13)}$ $p = 0.04$). *Col1a1* expression increases to a relative expression level close to 2 from e14 to primary cells, meaning that there is an increase in expression level when compared back to the control. (GLM, analysis of deviance $x^2_{(2,11)}$ $p = 0.082$). However, similarly to *Scx* this decreases as the cells are plated as a monolayer (p1), more similar with levels as E14 (Figure 3.6.1 c) but is relatively stable following this initial decrease from primary cells to p1 during passages (Figure 3.6.1 d). This is important as sometimes continued passaging is required to obtain enough cells for construct generation.

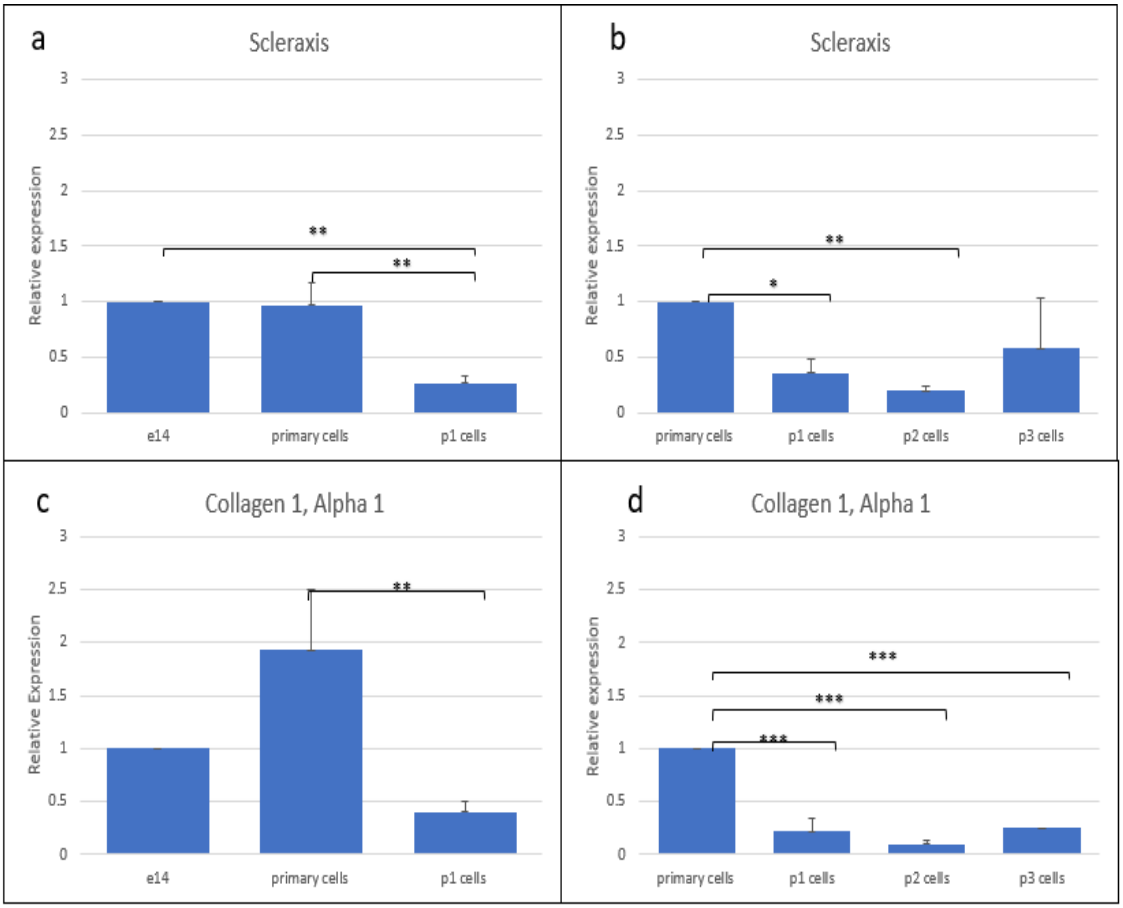

Figure 3.6.1 Molecular profile of relative expression of *chick collagen 1, alpha 1 (cCol1a1)* and *chick Scleraxis (cScx)* genes in native tendons (E14), and following purification of primary cells and following passages in culture (p1 to p3). a & c) indicate a comparison of relative expression of E14 tendon bundles to primary cells and cells expanded in culture, after the first passage (p1) cells. Expression levels were normalised to the housekeeping gene GAPDH and shown relative to expression in E14 tendon (set at 1). a) the relative expression of *scleraxis (Scx*) c) the relative expression of *collagen 1, alpha 1 (col1a1*). b) & d) compares the relative expression levels in Primary tenocyte cells and across cells after three passages (p1-3). Expression levels were normalised to the housekeeping gene GAPDH and shown relative to expression in primary cells (set to 1). b) relative expression of *scleraxis* (*Scx)*. d) the relative expression of *collagen 1, alpha 1 (col1a1*). N=5 experimental replicates with each gene run in triplicate. P values indicated as follows (*p ≤ 0.05, **p ≤ 0.01 ***p ≤ 0.001).

3.7 Collagen genes and tendon marker gene *scleraxis* are continually expressed in 'mini tendon' constructs.

To profile the changes of relative expression of Scleraxis (*Scx), Collagen 1, alpha 1(Col1a1), Collagen 3, alpha 1 (Col3a1) and Collagen 5, alpha 1 (Col5a1)* their relative expression levels were assessed by qRT-PCR from P3 cells (passage at which the constructs were plated from) to day 28 of culture to monitor changes in expression levels. These genes were chosen due to their role within tendon development. Relative expression of *Col1a1,* is shown in Figure 3.7.1 a, with stable expression across time in culture. The relative expression is 0.05 for day 9, when compared to the control which was set to 1 when normalised to p3 cells this indicates a decrease in expression from monolayer cells. Relative expression of *col3a1* is shown in Figure 3.7.1 b and across time in construct culture this remains fairly consistent, however with a lower level of expression at day 21 but shows a stabilisation at higher levels at day 28. Consistent expression of *col5a1* is shown in Figure 3.7.1 c, throughout time in culture. *Scx* expression shown in Figure 3.7.1d showing a similar pattern of consistent expression but contrariety to the collagen genes remains stable to monolayer expression at day 9 (value of 1) in this case before moderately lower levels at day 14 and increasing as time in culture progresses.

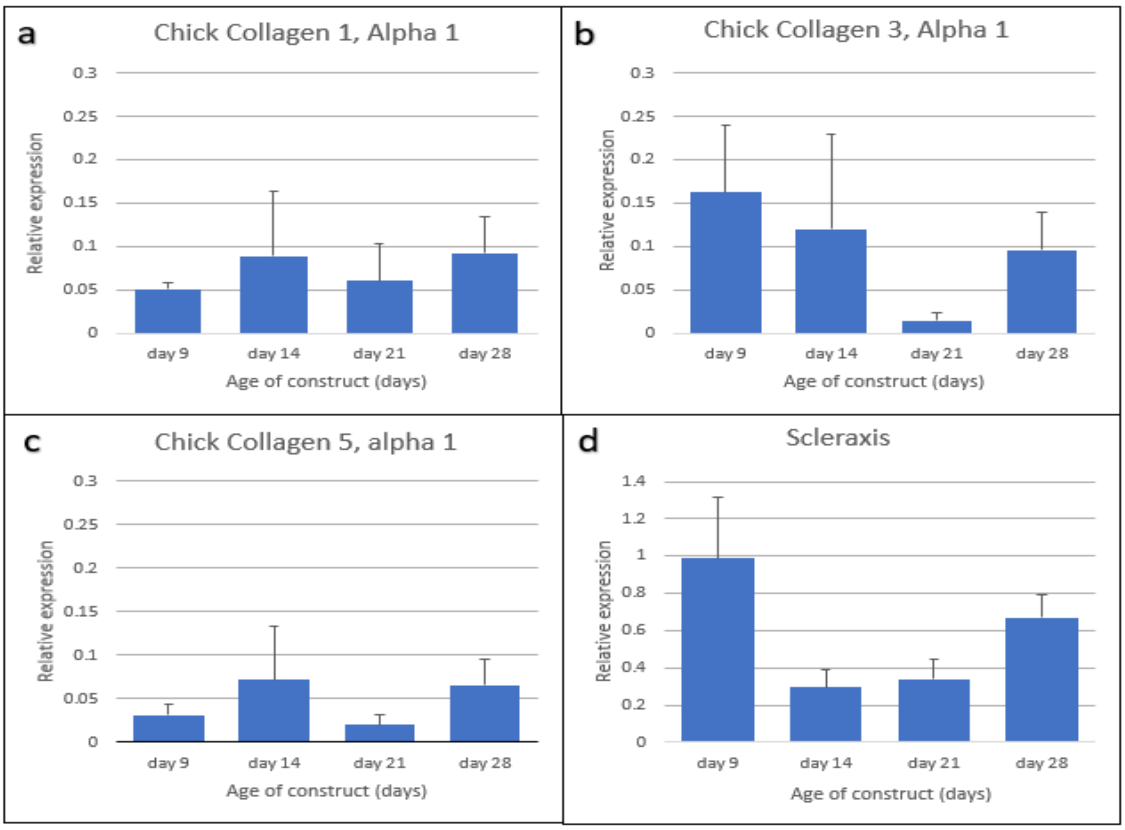

Figure 3.7.1. Molecular profile of relative expression of collagen genes and tendon marker gene within tissue engineered tendon constructs across time in culture from day 9 – day 28. Relative expression of; a) chick *collagen 1, alpha 1* (*cCol1a1*), b) chick *collagen 3, alpha 1 cCol3a1.* c) chick *collagen 5, alpha 1 (cCol5a1)* and d) *Scleraxis (Scx)*. Expression levels were normalised to the housekeeping gene GAPDH and shown relative to expression in p3 cells, passage at which the cells were used for construct plating (set to 1). N=4 experimental replicates for each, with each gene run in triplicate. A one-way ANOVA was carried out to determine significance of relative expression. A decrease when comparing constructs to the control (p3 cells, $p \leq 0.01$) for all genes shown above. No further statistical changes were found in any profile across time in construct culture.

4: Discussion

4.1 Project findings

In this study we show that primary tenocytes isolated from embryonic chick tendon are able to self-assemble as tendon-like constructs within a fibrin gel, across multiple experimental examples and timepoints. Analysis of the created constructs shows regions of collagen deposition, with collagen fibres that are aligned on the long axis of the constructs. Gene expression analysis showed that the mini-tendon constructs express collagen and tendon marker genes throughout their time in culture. This is a promising start to establish a system to test the mechanisms and pathways responsible for tendon development and maturation.

Through this study it was possible for embryonic chick tenocyte cells to self-assemble within a fibrin gel to produce mini-tendon constructs for 28 days in culture. The incorporation of the fibrin gel with cells is critical, as fibrin by itself does not initiate self-assembly, demonstrated by no rolling with experimental conditions without cells (see Figure 2.1.1 e). The tenocyte cells are able to self-assemble within both a fibrin and collagen gel however to encourage the environment whereby the tenocyte cells deposit their own collagen a fibrin gel has been shown to be more effective. (Yeung et al., 2015). Throughout time in culture tenocyte cells are able to deposit collagen, through the replacement of the fibrin with a thin filamentous matrix and then collagen fibrils (Breidenbach et al., 2015). Collagen is the main structural protein within connective tissues (Gelse, 2003, Thorpe and Screen, 2016) so its detection within the generated constructs is crucial.

Pan collagen binding protein (CNA35) (Mohammadkhah et al., 2017, Aper et al., 2014) was used in this study to visualise regions of collagen deposition within the tendon constructs. It has previously been used to visualise other developing tissues including metatarsal tendon tissue in the developing chick embryo (Peterson et al., 2021), as well as skeletal muscle tissue (Mohammadkhah et al., 2017). In native tissues collagen fibrils are visible as a clear collagen network of multiple fibres shown consistently throughout the tissue. The regions of collagen deposition found within the tendon constructs consisted of mostly central and peripheral clusters of high collagen deposition (see Figures 4.2.3 and 4.2.4). The use of CNA35 to visualise collagen within the *in vitro* constructs is novel, however the regions of high collagen deposition shown need to be replicated consistently throughout the tissue in order to produce a construct that resembles *in vivo* tissue. Therefore, the analysis and understanding of these regions of both high and low collagen deposition is the first step to achieve this, conditions

within high deposition need to be replicated and those responsible for low collagen need to be fully understood.

DAPI staining was used to visualise cell nuclei within the tendon constructs to determine the cell number located within regions of high collagen. Cell numbers were higher in regions of high collagen deposition for example within the day 9 constructs the average cell number in regions of high collagen deposition was 39 cells. Within regions of low collagen deposition this was decreased to 14 (One-way ANOVA, $F_{(1,4)} = 22674.3$, $p < 0.005$). (Figure 3.5.1). This is encouraging as cells deposit collagen from fibrin matrix (Breidenbach et al., 2015), although it is not exactly understood at this time what is it that causes these cells to accumulate in these regions which leads to high collagen deposition. We can speculate that tension from the experimental set up is a factor. Throughout time in culture the number of cells did not statistically increase (see Figure 3.5), which could be the reason as to why the regions of collagen deposition did not qualitatively increase over time (Figure 3.2.1). However interestingly, literature shows in previous studies that cell counts were maintained at a steady level until construct rolling, (day 7 in this case) and gradually decrease once the construct has fully rolled (Kalson et al., 2010). The variation in construct rolling showed variation from experiment to experiment, and within the same experiment (Figure 2.1.1 a-d). The point at which a construct is fully rolled is important to note as this affects lines of tension and alignment of collagen fibres throughout the construct. In this study we defined the analysis points from days of constrict plating (days 9,11,21 and 28), as the variation between experiments can be analysed and factors which affect this full rolling can be determined. However, in the Kadler lab protocol they define the day of rolling for individual constructs as T0 and begin analysis from this point to allow time for each construct to self-assemble within the gel (Kapacee et al., 2008, Yeung et al., 2015).

The alignment of pins and displacement of suture within the experimental setup was also shown to affect the ability of the tendon constructs to fully roll and self-assemble and therefore deposit collagen throughout. Displacement of the suture caused in all cases the construct to not fully roll (see Table 4.3.1). Although this incomplete rolling did not result in lack of collagen deposition (Figure 3.2.4 a, b and Figure 3.2.3 a, b), in some cases it did result in the lack of a consistent central region of collagen deposition throughout the centre of the construct (see Figure 3.2.3 b) compared to a fully rolled construct where collagen deposition is visible along the length of the construct (Figure 3.2.3 c). The reason for this could be that the movement of the suture disrupts the central line of tension created when the pins are fully aligned or that this movement creates multiple lines of tension which are weaker and

therefore do not cause the cells to deposit collagen in the same way. This tension is important as it has been shown through stress strain studies of tendon constructs that movement creates stronger, more robust tendons collagen fibril diameter and mechanical stiffness improved with the addition of this slow movement in culture (Kalson et al., 2011, Kalson et al., 2010) .

Birefringence was used to determine the alignment of collagen fibrils within tendon constructs, due to the highly organised structure of native collagen tissue aiming to be reproduced in this system. Collagen deposition is consistent along the long axis of the constructs, despite the angle of the pins not being consistently 180 degrees (Table 4.3.1). When the regions of high collagen deposition were spatially assessed there was a higher percentage of collagen fibres aligned in the central regions of the construct compared to peripheral regions of constructs that too showed deposition of high collagen (see Figure 3.4.2). This could be due to a line of tension created in the central portion of the construct, consistent with the alignment of pins. As the outside or edge of the construct is last to self-assemble it could therefore be under less tension if the construct does not fully roll. Initially the birefringence data was analysed for the whole construct together, with initial findings showing an unexpected decrease in collagen alignment over time. But with further analysis and separation of the data into central and peripheral spatial regions of collagen deposition, the distinct spatial organisation of the constructs were further demonstrated. Yeung et al, used serial block face-scanning electron microscopy (SBF-SEM), to visualise organisation of fibroblasts within the constructs (Yeung et al., 2015), and showed alignment along the long axis of the constructs, consistent with the results shown here for the birefringence studies (Figure 3.4.1 and 3.4.2). However, SBF-SEM does not allow for visualisation of types of collagen within the tissue to occur, and it has been shown that different types of collagens display different colours under polarised light (Coelho et al., 2018). Under polarised light mini tendon constructs consistently (Figure 3.4.1 c) displayed a yellow-green colour indicative of immature collagen type 1 and 3 fibres (Lopez De Padilla et al., 2021, Dayan et al., 1989). Relative expression data can be used to support findings surrounding the type of collagen tissue present within the constructs (see Figure 3.7.1), this supports the types of collagens observed through birefringence. Kalson et al, observed a significant increased in expression of tendon marker scleraxis from plating as a monolayer to construct and a further continued expression increase in culture until fully rolled (Kalson et al., 2010). The constructs produced *scleraxis* in this experiment continually during plating of cells as monolayers (Figure 3.7.1 d) but this decreased following construct plating and time in culture. It is not surprising that expression levels in this study do not match the literature as there are a number of

experimental adjustments that need to be further implemented from advice received and following protocol optimisation within the lab, but expression at this stage, even if not at high levels is encouraging.

4.2 Recommendations based upon learnings.

When establishing and optimising the protocol within the host lab I used a published protocol from the Kadler lab and based the protocol on these publications (Kalson et al., 2011, Kalson et al., 2010, Kapacee et al., 2008, Yeung et al., 2015). When comparing published results to results found within our analysis it was noted that there are some differences as have been outlined. Therefore, in order to further optimise the protocol and as, technical details within the published papers were limited. A member of the Kadler lab was contacted for advice to gain an insight into the more detailed steps to produce constructs that are fully self-assembled tendon like structures more consistently. The key differences are shown in Table 4.2.1 and indicate recommendations for the improvement of the experimental technique for further studies and continued protocol optimisation within the host lab, these recommendations also align with many of the findings and results produced in this study.

Table 4.2.1 Summary of protocol recommendations for future work based on completed experiments during this study.

Initial protocol used in the during this study	Recommendations for future experiments based on advice received and learnings from completed experiments
Using a stencil when placing pins and suture within the six well dish	Marking the base of each well within the six well plate using a ruler to ensure pins are completely parallel and aligned
2ml of Sylguard per well within each six well plate before addition of pins and suture	Thick layer of Sylguard (3-3.5ml per well) to provide a deeper base to anchor pins and pin down suture within each well to minimise risk of movement during the self-assembly process
Cell and fibrin mixture plated as thin cylinder surrounding two sets of pins and suture	Cell and fibrin mixture plated into centre of each well, followed by shaking the plate side to side to spread the mixture uniformly across whole surface allowing for the fibrin and gel to self-assemble over a number of days
Constructs plated at a density of $6.4x10^5$ cells per well	Increase cell seeding density to $7.5x10^5$ cells per well
Dissolving 1ml of fibrinogen at a time with PBS	Dissolving larger amounts of fibrinogen in media slowly (4hrs) filter sterilise and aliquot to make a stock solution

4.3 Further work and concluding remarks.

Alongside the Kadler Lab there have been other attempts to develop a tissue engineered solution to tendon injuries. The Arruda lab created a construct using cells isolated from a rat Achillies tendon and found that with mechanical stimulation the resulting construct resembled immature tendon tissue, that was able to in some cases be implanted *in vivo* and last a number of weeks (Calve et al., 2004, Calve et al., 2010). However, mechanisms with engineered tissue are difficult to reproduce and test especially in the capacity needed for clinical applications. Therefore, an alternative approach is suggested to understand the molecular and cellular pathways that are triggered by this mechanical stimulation with the idea to activate it in this way in order to generate mature tendon tissue *in vitro*. The host labs previous work has identified the importance of the WNT signalling pathway during development focusing on its downregulation during immobilisation (Rolfe et al., 2014), suggests it is a good candidate pathway to being with for pathway manipulation. YAP signalling is also being investigated as another candidate pathway within the host lab. YAP is a transcriptional regulator of the Hippo pathway (Dupont et al., 2011), which has been shown by the host lab to be responsive to mechanical regulation during the formation of the skeleton (Shea et al., 2020).

One way in which this genetic and cellular change that occurs during tendon maturation could be tested *in vitro* is through the use of Nanoparticle delivery, due to its highly translational and customisable properties. Nanoparticles are capable of delivering genetic cargo to a target cell or tissue without causing cell disruption or death (Auffan et al., 2009). A very effective and efficient type of nanoparticle known as RALA (Mccarthy et al., 2014), can be loaded with genetic cargo and result in the alteration in tissue properties such as levels of gene expression can be easily determined allowing the effects of specific genes and pathways to be determined. RALA has already been used successfully in a number of studies including gene therapy for cancer treatment in p3 prostate cancer cells (McCrudden et al., 2018). Nanoparticles could be incorporated within the fibrin gel set up at the point of construct plating slowly releasing genetic signals designed to achieve pathway manipulation. As this model system has the potential be manipulated and following the establishment of a good analysis pipeline, it will allow for the effects of pathway manipulation to be clearly determined.

A limitation of this study primarily involves the small sample size of experimental examples of the mini tendon constructs that have currently been fully analysed. This is due to issues that

arose during the processing and sectioning of constructs for both histological analysis and RNA extraction. This has resulted in the loss of sections in some cases and a lack of observation throughout all parts of a specimen, limiting the conclusions that can be drawn from a sample. In order to improve this timings and processing protocols have been tested and further optimised, due to the novel nature of the work these had not previously been tested.

The use of chick embryo cells in this tissue engineered model limits the direct translatability to human tissue engineering solutions. However, the knowledge and optimisations gleaned from this model can be applied to different cell types in the future. The more immediate value of this work is to develop a model system to test hypotheses of the biological mechanisms required to achieve consistent collagen deposition throughout and collagen fibril formation and ultimately maturation of tendon fibrils. In particular the aim is to use this system in the future for *in vitro* testing of signalling pathway manipulation. This would provide an opportunity to investigate different signalling pathways that play a role in tendon development and maturation. Beyond the use of tendon biology, the impact of being able to test and manipulate different signalling pathways, as the failure of a signalling pathway can lead to diseases, organ failure and cancer their full understanding is crucial for advancement in treating these problems.

5: References

ANDARAWIS-PURI, N., FLATOW, E. L. & SOSLOWSKY, L. J. 2015. Tendon basic science: Development, repair, regeneration, and healing. *Journal of Orthopaedic Research,* 33**,** 780-784.

APARECIDA DE ARO, A., DE CAMPOS VIDAL, B. & PIMENTEL, E. R. 2012. Biochemical and anisotropical properties of tendons. *Micron,* 43**,** 205-214.

APER, S. J. A., VAN SPREEUWEL, A. C. C., VAN TURNHOUT, M. C., VAN DER LINDEN, A. J., PIETERS, P. A., VAN DER ZON, N. L. L., DE LA RAMBELJE, S. L., BOUTEN, C. V. C. & MERKX, M. 2014. Colorful Protein-Based Fluorescent Probes for Collagen Imaging. *PLoS ONE,* 9**,** e114983.

AUFFAN, M., ROSE, J., BOTTERO, J. Y., LOWRY, G. V., JOLIVET, J. P. & WIESNER, M. R. 2009. Towards a definition of inorganic nanoparticles from an environmental, health and safety perspective. *Nature Nanotechnology,* 4**,** 634-641.

BASS, L. E. 2012. Tendinopathy: Why the Difference Between Tendinitis and Tendinosis Matters. *International Journal of Therapeutic Massage & Bodywork: Research, Education, & Practice,* 5.

BERGAMIN, F., CIVERA, M., RODRIGUEZ REINOSO, M., BURGIO, V., RUIZ, O. G. & SURACE, C. 2023. Worldwide Incidence and Surgical Costs of Tendon Injuries: A Systematic Review and Meta-Analysis. *Muscle Ligaments and Tendons Journal,* 13.

BIRK, D. E., NURMINSKAYA, M. V. & ZYCBAND, E. I. 1995. Collagen fibrillogenesis in situ: Fibril segments undergo post-depositional modifications resulting in linear and lateral growth during matrix development. *Developmental Dynamics,* 202**,** 229-243.

BOBZIN, L., ROBERTS, R. R., CHEN, H.-J., CRUMP, J. G. & MERRILL, A. E. 2021. Development and maintenance of tendons and ligaments. *Development,* 148.

BREIDENBACH, A. P., DYMENT, N. A., LU, Y., RAO, M., SHEARN, J. T., ROWE, D. W., KADLER, K. E. & BUTLER, D. L. 2015. Fibrin Gels Exhibit Improved Biological, Structural, and Mechanical Properties Compared with Collagen Gels in Cell-Based Tendon Tissue-Engineered Constructs. *Tissue Engineering Part A,* 21**,** 438-450.

BUTLER, D. L., GOOCH, C., KINNEBERG, K. R. C., BOIVIN, G. P., GALLOWAY, M. T., NIRMALANANDHAN, V. S., SHEARN, J. T., DYMENT, N. A. & JUNCOSA-MELVIN, N. 2010. The use of mesenchymal stem cells in collagen-based scaffolds for tissue-engineered repair of tendons. *Nature protocols,* 5**,** 849-863.

CALVE, S., DENNIS, R. G., KOSNIK, P. E., BAAR, K., GROSH, K. & ARRUDA, E. M. 2004. Engineering of Functional Tendon. *Tissue Engineering,* 10**,** 755-761.

CALVE, S., LYTLE, I. F., GROSH, K., BROWN, D. L. & ARRUDA, E. M. 2010. Implantation increases tensile strength and collagen content of self-assembled tendon constructs. *J Appl Physiol (1985),* 108**,** 875-81.

CHARTIER, C., ELHAWARY, H., BARADARAN, A., VORSTENBOSCH, J., XU, L. & EFANOV, J. I. 2021. Tendon: Principles of Healing and Repair. *Seminars in plastic surgery,* 35(3)**,** 211–215.

CHEN, J., XU, J., WANG, A. & ZHENG, M. 2009. Scaffolds for tendon and ligament repair: review of the efficacy of commercial products. *Expert Review of Medical Devices,* 6**,** 61-73.

CHO, J., LEE, H., RAH, W., CHANG, H. J. & YOON, Y.-S. 2022. From engineered heart tissue to cardiac organoid. *Theranostics,* 12**,** 2758-2772.

COELHO, P. G. B., SOUZA, M. V. D., CONCEIÇÃO, L. G., VILORIA, M. I. V. & BEDOYA, S. A. O. 2018. Evaluation of dermal collagen stained with picrosirius red and examined under polarized light microscopy. *Anais Brasileiros de Dermatologia,* 93**,** 415-418.

DAYAN, D., HISS, Y., HIRSHBERG, A., BUBIS, J. J. & WOLMAN, M. 1989. Are the polarization colors of Picrosirius red-stained collagen determined only by the diameter of the fibers? *Histochemistry,* 93**,** 27-29.

DUPONT, S., MORSUT, L., ARAGONA, M., ENZO, E., GIULITTI, S., CORDENONSI, M., ZANCONATO, F., LE DIGABEL, J., FORCATO, M., BICCIATO, S., ELVASSORE, N. & PICCOLO, S. 2011. Role of YAP/TAZ in mechanotransduction. *Nature,* 474**,** 179-184.

FELSENTHAL, N. & ZELZER, E. 2017. Mechanical regulation of musculoskeletal system development. *Development,* 144**,** 4271-4283.

GALLOWAY, M. T., LALLEY, A. L. & SHEARN, J. T. 2013. The Role of Mechanical Loading in Tendon Development, Maintenance, Injury, and Repair. *Journal of Bone and Joint Surgery,* 95**,** 1620-1628.

GEHWOLF, R., SPITZER, G., WAGNER, A., LEHNER, C., WEISSENBACHER, N., TEMPFER, H. & TRAWEGER, A. 2019. 3D-Embedded Cell Cultures to Study Tendon Biology. *Methods Mol Biol,* 2045**,** 155-165.

GELSE, K. 2003. Collagens—structure, function, and biosynthesis. *Advanced Drug Delivery Reviews,* 55**,** 1531-1546.

HAMBURGER, V. & HAMILTON, H. L. 1992. A SERIES OF NORMAL STAGES IN THE DEVELOPMENT OF THE CHICK EMBRYO. *DEVELOPMENTAL DYNAMICS,* 88**,** 195231-272.

HESS, G. P., CAPPIELLO, W. L., POOLE, R. M. & HUNTER, S. C. 1989. Prevention and Treatment of Overuse Tendon Injuries. *Sports Medicine,* 8**,** 371-384.

HOFER, M. & LUTOLF, M. P. 2021. Engineering organoids. *Nature Reviews Materials,* 6**,** 402-420.

JELINSKY, S. A., RODEO, S. A., LI, J., GULOTTA, L. V., ARCHAMBAULT, J. M. & SEEHERMAN, H. J. 2011. Regulation of gene expression in human tendinopathy. *BMC Musculoskeletal Disorders,* 12**,** 86.

KALSON, N. S., HOLMES, D. F., HERCHENHAN, A., LU, Y., STARBORG, T. & KADLER, K. E. 2011. Slow stretching that mimics embryonic growth rate stimulates structural and mechanical development of tendon-like tissue in vitro. *Developmental Dynamics,* 240**,** 2520-2528.

KALSON, N. S., HOLMES, D. F., KAPACEE, Z., OTERMIN, I., LU, Y., ENNOS, R. A., CANTY-LAIRD, E. G. & KADLER, K. E. 2010. An experimental model for studying the biomechanics of embryonic tendon: Evidence that the development of mechanical properties depends on the actinomyosin machinery. *Matrix Biology,* 29**,** 678-689.

KANNUS, P. 2000. Structure of the tendon connective tissue. *Scandinavian Journal of Medicine & Science in Sports,* 10**,** 312-320.

KAPACEE, Z., RICHARDSON, S. H., LU, Y., STARBORG, T., HOLMES, D. F., BAAR, K. & KADLER, K. E. 2008. Tension is required for fibripositor formation. *Matrix Biology,* 27**,** 371-375.

KARDON, G. 1998. Muscle and tendon morphogenesis in the avian hind limb. *Development,* 125**,** 4019-4032.

KIRKENDALL, D. T. & GARRETT, W. E. 1997. Function and biomechanics of tendons. *Scandinavian Journal of Medicine & Science in Sports,* 7**,** 62-66.

KVIST, M. H., LEHTO, M. U. K., JOZSA, L., JÄRVINEN, M. & KVIST, H. T. 1988. Chronic Achilles paratenonitis: An immunohistologic study of fibronectin and fibrinogen. *The American Journal of Sports Medicine,* 16**,** 616-623.

LOPEZ DE PADILLA, C. M., COENEN, M. J., TOVAR, A., DE LA VEGA, R. E., EVANS, C. H. & MULLER, S. A. 2021. Picrosirius Red Staining: Revisiting Its Application to the Qualitative and Quantitative Assessment of Collagen Type I and Type III in Tendon. *J Histochem Cytochem,* 69**,** 633-643.

LUI, P. P. 2015. Stem cell technology for tendon regeneration: current status, challenges, and future research directions. *Stem Cells and Cloning: Advances and Applications***,** 163.

MCBRIDE, D. J., TRELSTAD, R. L. & SILVER, F. H. 1988. Structural and mechanical assessment of developing chick tendon. *International Journal of Biological Macromolecules,* 10**,** 194-200.

MCCARTHY, H. O., MCCAFFREY, J., MCCRUDDEN, C. M., ZHOLOBENKO, A., ALI, A. A., MCBRIDE, J. W., MASSEY, A. S., PENTLAVALLI, S., CHEN, K. H., COLE, G., LOUGHRAN, S. P., DUNNE, N. J., DONNELLY, R. F., KETT, V. L. & ROBSON, T. 2014. Development and characterization of self-assembling nanoparticles using a bio-inspired amphipathic peptide for gene delivery. *Journal of Controlled Release,* 189**,** 141-149.

MCCRUDDEN, C. M., MCBRIDE, J. W., MCCAFFREY, J., MCERLEAN, E. M., DUNNE, N. J., KETT, V. L., COULTER, J. A., ROBSON, T. & MCCARTHY, H. O. 2018. Gene therapy with RALA/iNOS composite nanoparticles significantly enhances survival in a model of metastatic prostate cancer. *Cancer Nanotechnology,* 9.

MILLAR, N. L., SILBERNAGEL, K. G., THORBORG, K., KIRWAN, P. D., GALATZ, L. M., ABRAMS, G. D., MURRELL, G. A. C., MCINNES, I. B. & RODEO, S. A. 2021. Tendinopathy. *Nature Reviews Disease Primers,* 7**,** 1.

MOHAMMADKHAH, M., SIMMS, C. K. & MURPHY, P. 2017. Visualisation of Collagen in fixed skeletal muscle tissue using fluorescently tagged Collagen binding protein CNA35. *Journal of the Mechanical Behavior of Biomedical Materials,* 66**,** 37-44.

PETERSON, B. E., ROLFE, R. A., KUNSELMAN, A., MURPHY, P. & SZCZESNY, S. E. 2021. Mechanical Stimulation via Muscle Activity Is Necessary for the Maturation of Tendon Multiscale Mechanics During Embryonic Development. *Frontiers in Cell and Developmental Biology,* 9.

RAWSON, S., CARTMELL, S. & WONG, J. 2013. Suture techniques for tendon repair; a comparative review. *Muscles, ligaments and tendons journal,* 3 (3)**,** 220 - 228.

RILEY, G. 2003. The pathogenesis of tendinopathy. A molecular perspective. *Rheumatology,* 43**,** 131-142.

RODDY, K. A., NOWLAN, N. C., PRENDERGAST, P. J. & MURPHY, P. 2009. 3D representation of the developing chick knee joint: a novel approach integrating multiple components. *Journal of Anatomy,* 214**,** 374-387.

RODRIGUES, M. T., REIS, R. L. & GOMES, M. E. 2013. Engineering tendon and ligament tissues: present developments towards successful clinical products: Engineering tendon and ligament tissues. *Journal of Tissue Engineering and Regenerative Medicine,* 7**,** 673-686.

ROLFE, R. A., NOWLAN, N. C., KENNY, E. M., CORMICAN, P., MORRIS, D. W., PRENDERGAST, P. J., KELLY, D. & MURPHY, P. 2014. Identification of mechanosensitive genes during skeletal development: Alteration of genes associated with cytoskeletal rearrangement and cell signalling pathways. *BMC Genomics,* 15.

RUIZ-ALONSO, S., LAFUENTE-MERCHAN, M., CIRIZA, J., SAENZ-DEL-BURGO, L. & PEDRAZ, J. L. 2021. Tendon tissue engineering: Cells, growth factors, scaffolds and production techniques. *Journal of Controlled Release,* 333**,** 448-486.

SCHWEITZER, R., ZELZER, E. & VOLK, T. 2010. Connecting muscles to tendons: tendons and musculoskeletal development in flies and vertebrates. *Development,* 137**,** 2807-2817.

SHEA, C. A., ROLFE, R. A., MCNEILL, H. & MURPHY, P. 2020. Localization of YAP activity in developing skeletal rudiments is responsive to mechanical stimulation. *Developmental Dynamics,* 249**,** 523-542.

SKARDAL, A., DEVARASETTY, M., RODMAN, C., ATALA, A. & SOKER, S. 2015. Liver-Tumor Hybrid Organoids for Modeling Tumor Growth and Drug Response In Vitro. *Annals of Biomedical Engineering,* 43**,** 2361-2373.

TANG, X.-Y., WU, S., WANG, D., CHU, C., HONG, Y., TAO, M., HU, H., XU, M., GUO, X. & LIU, Y. 2022. Human organoids in basic research and clinical applications. *Signal Transduction and Targeted Therapy,* 7.

THORPE, C. T. & SCREEN, H. R. C. 2016. Tendon Structure and Composition. *Advances in Experimental Medicine and Biology (AEMB,volume 920).* Springer International Publishing.

VASILIADIS, A. V. & KATAKALOS, K. 2020. The Role of Scaffolds in Tendon Tissue Engineering. *Journal of Functional Biomaterials,* 11**,** 78.

WALDEN, G., LIAO, X., DONELL, S., RAXWORTHY, M. J., RILEY, G. P. & SAEED, A. 2017. A Clinical, Biological, and Biomaterials Perspective into Tendon Injuries and Regeneration. *Tissue Engineering Part B: Reviews,* 23**,** 44-58.

WANG, J. H. C. 2006. Mechanobiology of tendon. *Journal of Biomechanics,* 39**,** 1563-1582.

YEUNG, C. Y. C., ZEEF, L. A. H., LALLYETT, C., LU, Y., CANTY-LAIRD, E. G. & KADLER, K. E. 2015. Chick tendon fibroblast transcriptome and shape depend on whether the cell has made its own collagen matrix. *Scientific Reports,* 5.

ZHANG, H., WANG, M., WU, R., GUO, J., SUN, A., LI, Z., YE, R., XU, G. & CHENG, Y. 2023. From materials to clinical use: advances in 3D-printed scaffolds for cartilage tissue engineering. *Physical Chemistry Chemical Physics,* 25**,** 24244-24263.